PHYSICAL REVIEW C
NUCLEAR PHYSICS

THIRD SERIES, VOLUME 27, NUMBER 5 — MAY 1983

Proton capture to excited states of ^{16}O: $M1$, $E1$, and Gamow-Teller transitions and shell model calculations

K. A. Snover and E. G. Adelberger
Nuclear Physics Laboratory, University of Washington, Seattle, Washington 98195
and Nuclear Physics Laboratory, Oxford University, Oxford OX1 3RH, England

P. G. Ikossi
Nuclear Physics Laboratory, University of Washington, Seattle, Washington 98195

B. A. Brown
Nuclear Physics Laboratory, Oxford University, Oxford OX1 3RH, England
and Cyclotron Laboratory, Michigan State University, East Lansing, Michigan 48824

(Received 25 January 1983)

We have measured excitation functions of the γ rays resulting from the bombardment of ^{15}N by polarized and unpolarized protons in the energy range $E_p=2.5$–9.5 MeV with emphasis on identifying dipole decays to the first (0^+) and second (3^-) excited states in ^{16}O. Resonances in γ_{12} are observed at $E_x=16.21$, 16.45, 16.82, 17.12, 18.03, 18.98, 19.90, and 20.41 MeV. The 16.21 and 17.12 MeV resonances in γ_{12} are identified as $M1$ decays of the 1^+ $T=1$ states to the 6.05 MeV 0^+ state in ^{16}O. The measured ratio of reduced strengths $B(M1,\gamma_1)/B(M1,\gamma_0)$ is 0.48 ± 0.03 for decays from the 16.21 MeV state and 0.55 ± 0.04 for decays from the 17.12 MeV state. The 18.03 MeV resonance is due to a 3^- $T=1$ state in ^{16}O with a strength $\Gamma_p\Gamma_{\gamma_2}/\Gamma=(1.96\pm0.27)$ eV and the 18.98 MeV resonance is due to the 4^- $T=1$ stretched particle-hole state with a strength of (0.85 ± 0.10) eV. We determine absolute particle and γ widths for these states. The $M1$ γ_2 width of the 18.98 MeV state, (7.1 ± 3.1) eV, is in agreement with a shell-model calculation. Resonances in γ_3 are observed at 16.82 and 17.27 MeV and in γ_4 at 17.88 MeV. The excitation energies and widths of these levels as well as the strengths of the γ transitions suggest a $T=1$ character for all of the resonances for which capture γ rays are observed. Correspondences of our resonances to levels in ^{16}N are given. Strong α_1 branches for many of these states indicate isospin impurities. We compare γ widths, including ground-state $M1$ decays, and allowed β transition rates in $A=16$ nuclei with shell model calculations and obtain rough agreement with the experimental results. Additional shell model calculations for $M1$ and Gamow-Teller decays in the $A=14$, 15, 17, and 18 nuclei are presented, which indicate that Gamow-Teller matrix elements are quenched by $\sim20\%$ relative to shell model predictions and also relative to the spin part of the $M1$ matrix elements.

[NUCLEAR REACTIONS ^{15}N$(p,\gamma)^{16}$O, ^{15}N$(p,p'\gamma)^{15}$N, ^{15}N$(p,\alpha_1\gamma)^{12}$C, $E=2.5$–9.5 MeV, measured capture γ rays to $E_x=6.05$, 6.13, 6.92, and 7.12 MeV final states. Measured $\sigma(90°)$, $A_y(90°)$, $\sigma(\theta)$. Deduced $M1$ and $E1$ resonance strengths. Performed shell model calculations and compared with these and other $M1$ and Gamow-Teller strengths in nuclei near $A=16$. Deduced average inhibition of GT matrix elements relative to shell model and to the spin part of $M1$ matrix elements.]

I. INTRODUCTION

The well-known and very impressive successes of the many-particle shell model have contributed greatly to our confidence that we can achieve a predictive theory of nuclear structure. In particular the calculations of Cohen and Kurath[1] in the $0p$ shell and of Wildenthal and collaborators[2] in the $1s0d$ shell have shown that a vast amount of spectroscopic data can be successfully explained by a relatively small number of parameters (single-particle energies and residual two-body matrix elements) which are chosen to fit the results and found to have "reasonable" values.

However, it must be appreciated that these successes are triumphs of the $0\hbar\omega$ shell model, i.e., a model in which the basis vectors, although in general very complex, are restricted to lie within a single major shell. This basis is expected to be sufficient for describing $M1$ and allowed Gamow-Teller decays where operators only connect configurations lying within a major shell. This expectation is confirmed. On the other hand, matrix elements of operators which cross major shells as well as connecting configurations within a major shell are not expected to be given correctly by the $0\hbar\omega$ shell model. Examples are $E2$ γ transitions and second forbidden β decay. These must be treated phenomenologically; for example, by endowing the neutron and proton with effective charges. This procedure often gives reasonable results.

In view of all these achievements it is perhaps surprising that the shell model has met with such limited quantitative success in accounting for quantities which vanish in a $0\hbar\omega$ basis and manifestly require $1\hbar\omega$, $2\hbar\omega$, etc., excitations. Examples are unnatural parity states; $E1$, $M2$, or $E3$ transitions; or $M1$ transitions in a "closed-shell" nucleus. Upon closer examination, however, it is clear that a formidable problem is encountered as one expands the basis from $0\hbar\omega$ to $n\hbar\omega$. In order to completely exclude spurious center-of-mass (c.m.) motion in the eigenvectors one needs a basis which spans the complete $n\hbar\omega$ space. The resulting model spaces are enormous. Nevertheless, improvements in computational techniques and intelligent truncation schemes offer hope that the problem can be solved. Our need to understand nuclear structure compels us to attempt the task.

The ^{16}O nucleus plays a very important role in attempts to refine the multi-$\hbar\omega$ shell model since in the $0\hbar\omega$ approximation ^{16}O would have no excited states. The $M1\gamma$ decay and Gamow-Teller β decay transitions provide a particularly clean test of shell model wave functions since the operators are well understood and have no radial dependence in the long-wavelength limit. For example, the recent identification[3] of magnetic-dipole $(M1)\gamma$-transition strength built on the ground state of ^{16}O provides a direct measure of the $2\hbar\omega$, $4\hbar\omega$, etc., correlations in the ground-state wave function. Because the $M1$ operator has no radial dependence in the long wavelength approximation, it cannot excite the closed shell component of the ground state wave function. A similar argument applies to the $M1$ decays to the excited 0^+ states. Only the 2p-2h and 4p-4h components of the 1^+ and 0_2^+ states can contribute to the $M1$ transition strength between these states. Thus a measurement of the relative $M1$ strength for decay of the 1^+ $T=1$ levels to the various 0^+ $T=0$ states severely constrains shell model calculations of the wave functions of the 1^+ initial states and the 0^+ final states.

In this paper we report on experimental studies of γ-ray observables in ^{16}O with particular emphasis on $M1$ transitions connecting the 1^+ $T=1$ states to the 0_2^+ $T=0$ level and on $M1$ transitions deexciting the 3^- $T=1$ state at 18.03 MeV and the 4^- $T=1$ 18.98 MeV state in ^{16}O. Other resonances observed in our excitation functions are also discussed. The excitation energies, widths, spins, and γ-ray widths of most of the states observed in this work suggest that they are analogs of known levels in ^{16}N. On the other hand, isospin impurities in these levels are revealed by finite widths for α decay.

We conclude by comparing measured $M1$ and Gamow-Teller (GT) matrix elements to shell model calculations in the mass 14, 15, 16, 17, and 18 nuclei. We discuss problems associated with large-basis shell model calculations around $A=16$ and identify shortcomings in some commonly used truncation schemes and residual interactions. We show that GT matrix elements are on the average inhibited by about 20% relative to shell-model predictions, and that an inhibition of similar magnitude exists for GT matrix elements compared to the spin part of $M1$ matrix elements.

II. EXPERIMENTAL PROCEDURE

The experiments were performed with the University of Washington FN tandem accelerator. Gamma rays from proton capture were detected in a 25×25 cm NaI spectrometer with an anticoincidence shield. We used a polarized beam to measure the excitation functions at $\theta_\gamma=90°$ for proton energies between 6.2 and 9.1 MeV (Figs. 1–3). The data below 7.4 MeV in Fig. 1 were taken with a ^{15}N (99.9% purity) gas target (0.3 mg/cm^2) with Ni entrance (0.6 mg/cm^2) and exit foils. At higher energies a thicker ^{15}N tar-

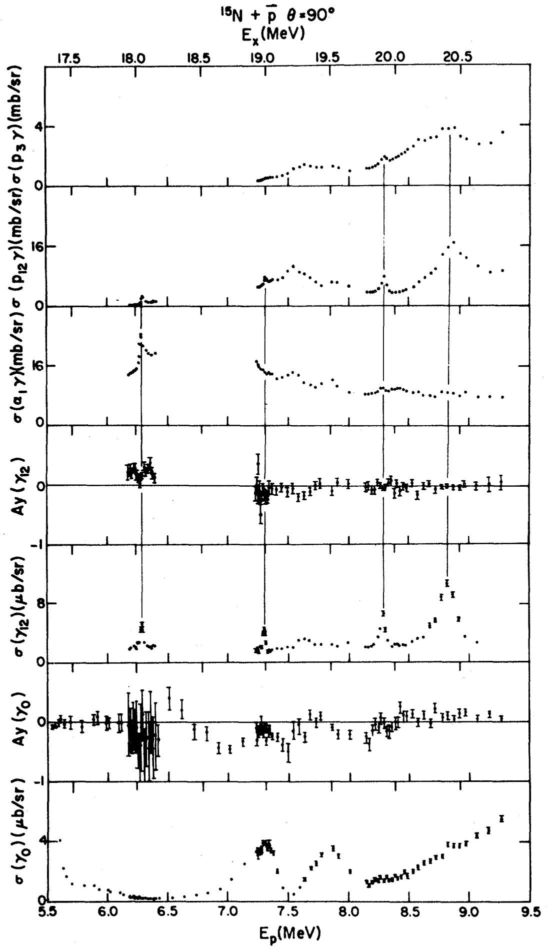

FIG. 1. Excitation functions at $\theta_\gamma=90°$ for the ^{15}N$(p,\gamma_0)^{16}$O, ^{15}N$(p,\gamma_{12})^{16}$O ($E_x=6.05$, 6.13 MeV), ^{15}N$(p,\alpha_1\gamma)^{12}$C, ^{15}N$(p,p_{12}\gamma)^{15}$N, and ^{15}N$(p,p_3\gamma)^{15}$N reactions measured using a gas target.

get (0.64 mg/cm^2) and thicker Ni foils (0.9 mg/cm^2) were used. Under these conditions, we obtained high-quality yield curves for the γ_0 and γ_{12} decays. However, the γ_{34} transitions occurred in an energy range obscured by γ rays from the Ni foil. Using an unpolarized proton beam and a ^{15}N-enriched (99%) melamine target we measured 90° excitation functions for incident energies between 2.5 and 6.3 MeV (Fig. 4). At energies greater than 4.0 MeV the γ_{34} cross sections could be extracted from the melamine data. Below $E_p=4.0$ MeV the γ rays from primary and secondary decays involving the 8.88 MeV level in ^{16}O fall in the same energy range as the capture γ rays of interest and it becomes difficult to extract γ_{12} and γ_{34} yields. Below the neutron threshold the spectra become very clean, and one can identify both the primary and secondary γ rays of the decays to the excited states of ^{16}O. We do not see any sharp resonances in the γ_0 and γ_{12} excitation functions between $E_p=2.6$ and 4.0 MeV, although pileup from the intense 4.4 MeV γ rays obscures the region of the excitation function near $E_p=3$ MeV. Additional polarized-beam data on the $E_x=18.98$ MeV and $E_x=18.03$ MeV resonances (Figs. 2 and 3) were taken using the melamine target ($C_3H_6{}^{15}N_6 \sim 0.29$ mg/cm^2).

Information on the γ rays from the α_1, p_{12}, and p_3 exit channels was obtained by digitizing the lower energy part of the γ-ray spectrum in a second analog-to-digital converter (ADC). This second spectrum was prescaled by a factor of 10 and did not have the anticoincidence requirement from the plastic shield surrounding the NaI.

III. DATA ANALYSIS

Areas of the gamma ray peaks were extracted by fitting experimentally deduced line shapes to the spectra. No background subtraction was necessary for the capture γ rays. For the reaction γ rays an empirical background line shape determined at bombarding energies below the p_{12} threshold was used. Typical spectra with the corresponding fits are shown in Fig. 5.

In fitting the spectra, the relative separation of the observed lines was fixed by the known energy differences of the final states. The width of the line shape for the capture γ rays was assumed to increase linearly with energy, whereas for the reaction γ rays the width was kept constant. The absolute normalization ($\pm 10\%$) of the capture γ-ray data was deduced by normalizing the γ_0 yields to our previously measured[3] absolute cross section of 3.75 ± 0.26 μb/sr at $E_p=7.30$ MeV. A 3% per MeV correction was applied to the measured yields to account for the decrease in the detection efficiency with increasing γ-ray energy. The agreement between our γ_0 data and those of Ref. 3 is very good. The γ_0 and γ_{12} data are also in good qualitative agreement with those of Refs. 4 and 5. Our data overlap those of Barnett *et al.*[6] Although our work agrees with Ref. 6 for $E_p \geq 6$ MeV, there is strong disagreement below 6 MeV, where our γ_{12} cross sections are smaller than those of Ref. 6. This indicates that the data of Ref. 6 below $E_p=6.0$ MeV are dominated by strong background contributions.

The normalization of the reaction γ-rays cross sections was obtained using the relative efficiency of our NaI at 4.4 and 15.1 MeV given in Ref. 7. This procedure introduced an additional uncertainty of

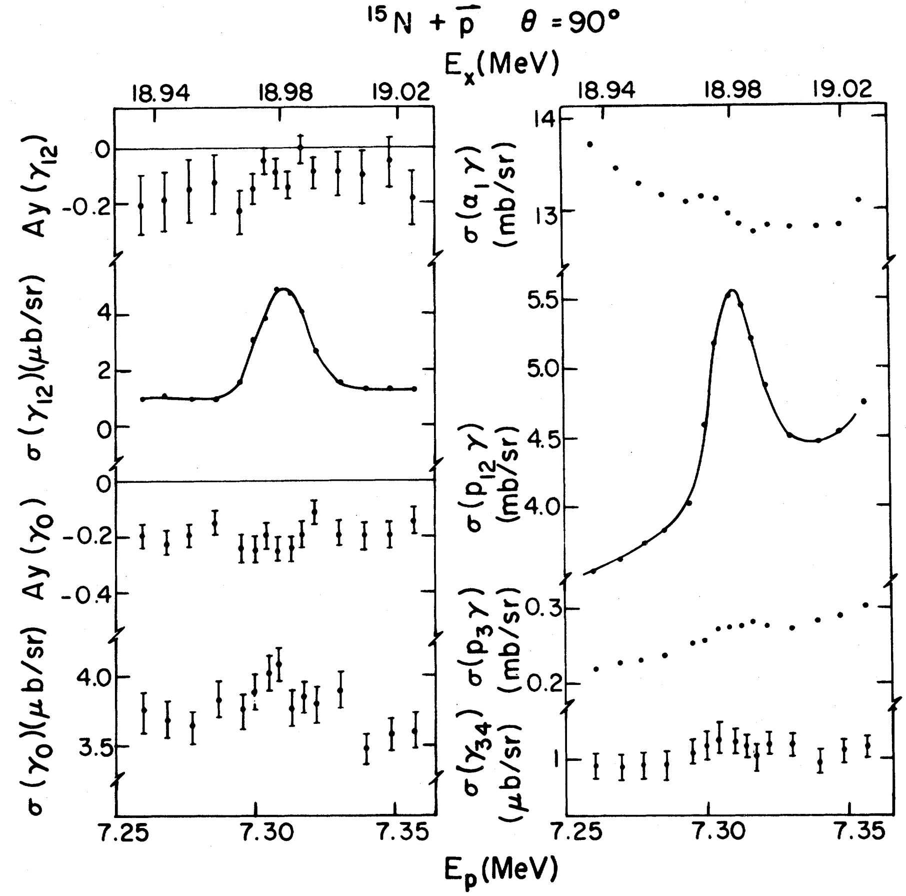

FIG. 2. Excitation functions in the vicinity of the 18.98 MeV 4^- state taken with a melamine target.

$\pm15\%$ in the absolute cross sections for the reaction γ rays. Absolute yields were extracted independently for the gas cell and melamine target data. With the melamine target, both the $^{15}N(p,\alpha_1\gamma)^{12}C$ and the $^{12}C(p,p_1\gamma)^{12}C$ reactions contributed to the yield of the 4.43 MeV γ rays. In the region between 6.3 and 7.3 MeV the contribution of the $^{12}C(p,p_1\gamma)$ reaction[8] is estimated to be 15% of the observed cross section. Our normalized data for the gas and melamine targets agree to within $\pm10\%$, consistent within the uncertainties in the absolute normalization, except for the off resonance cross sections for the 5.3 MeV γ rays at $E_p \sim 7.3$ MeV, which differ by $\sim 20\%$. Resonance strengths deduced from the melamine and the gas cell data are consistent, indicating that the higher yield of 5.3 MeV γ rays in the gas cell data is due to an unidentified contaminant background which is absent in the melamine data. The overall uncertainty in the absolute normalization of the reaction data is estimated to be $\pm20\%$.

IV. RESULTS

In this section we discuss the resonance structures observed in our excitation functions. All proton resonance energies are given in the laboratory system and correspond to the energy in the center of the target. Resonance widths are in the center-of-mass system. Total widths were estimated from the observed widths and the energy loss in the target. The latter was determined from a comparison of the observed width and the total width of the 18.98 MeV resonance (see Sec. IV C). We assumed that the energy loss in the target and the width of the state contribute quadratically to the observed width, and we included the variation in the energy loss in the target as a function of proton beam energy.

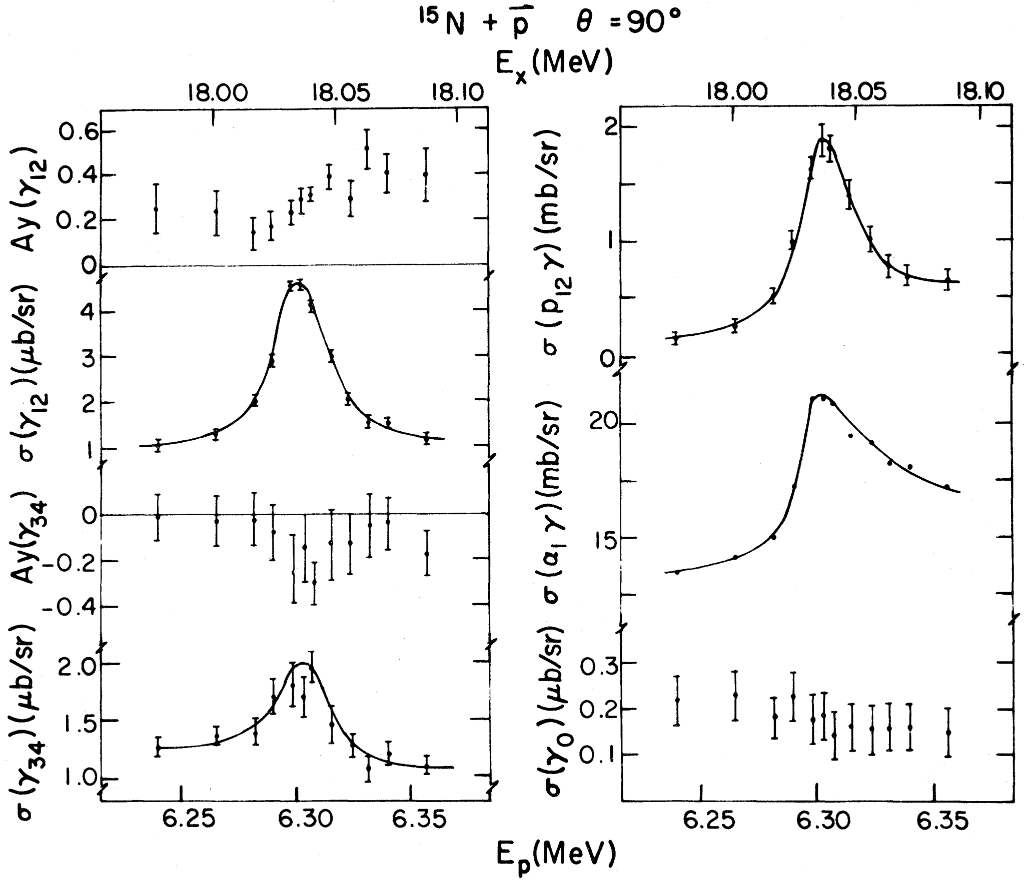

FIG. 3. Excitation functions in the vicinity of the 18.03 MeV 3^- state taken with a melamine target.

A. Assumptions of the analysis

Gamma decay widths are inferred from the measured (p,γ) cross section at $\theta=90°$ and the measured a_2 coefficients of the angular distributions. When the latter were not available we estimated the gamma strength using theoretical values (see Table I) for the a_2 coefficient.

Particle and γ decay widths to excited residual states were deduced by assuming that resonance-background interference in the γ-ray excitation functions can be neglected. For the $E_x=18.03$ and 18.98 MeV resonances we use measured angular distributions to extract the absolute strengths. For the other particle-decay resonances we assume isotropic resonance angular distributions. When values for Γ_{n_0} could not be inferred from previous work we assumed the isospin symmetric relation $\gamma_n{}^2=\gamma_p{}^2$. We define $\gamma_N{}^2$ by $\Gamma_N=2P\gamma_N{}^2$, where P is a penetrability calculated for the lowest allowed l value and

$$R=r_0(A_1{}^{1/3}+A_2{}^{1/3})$$

with $r_0=1.35$ fm. The branching ratios Γ_{p_0}/Γ, when not known from previous work, were determined by requiring that $\Sigma\Gamma_x=\Gamma$ assuming that, in addition to n_0 and p_0, only the observed channels contribute to the sum (see Table V). This leads to a quadratic equation for each resonance, with two possible solutions. We used the mean of these two solutions for our estimate of Γ_{p_0}/Γ in Table V. For all cases the individual solutions were within $\pm 35\%$ of the mean, except for the $E_x=17.880$ MeV resonance, for which the two solutions for Γ_{p_0}/Γ are 0.09 and 0.63. Although we quote errors on the resonance strengths, in Table V we do not give errors on the extracted values of the radiative widths because it is difficult to assess the uncertainties in our estimates of Γ_{p_0}/Γ. A future measurement of these proton branching ratios by coincidence techniques would be valuable.

Limits on the resonance spins are deduced by assuming dipole decays for the capture γ rays. This is based on the empirical observation that for states of

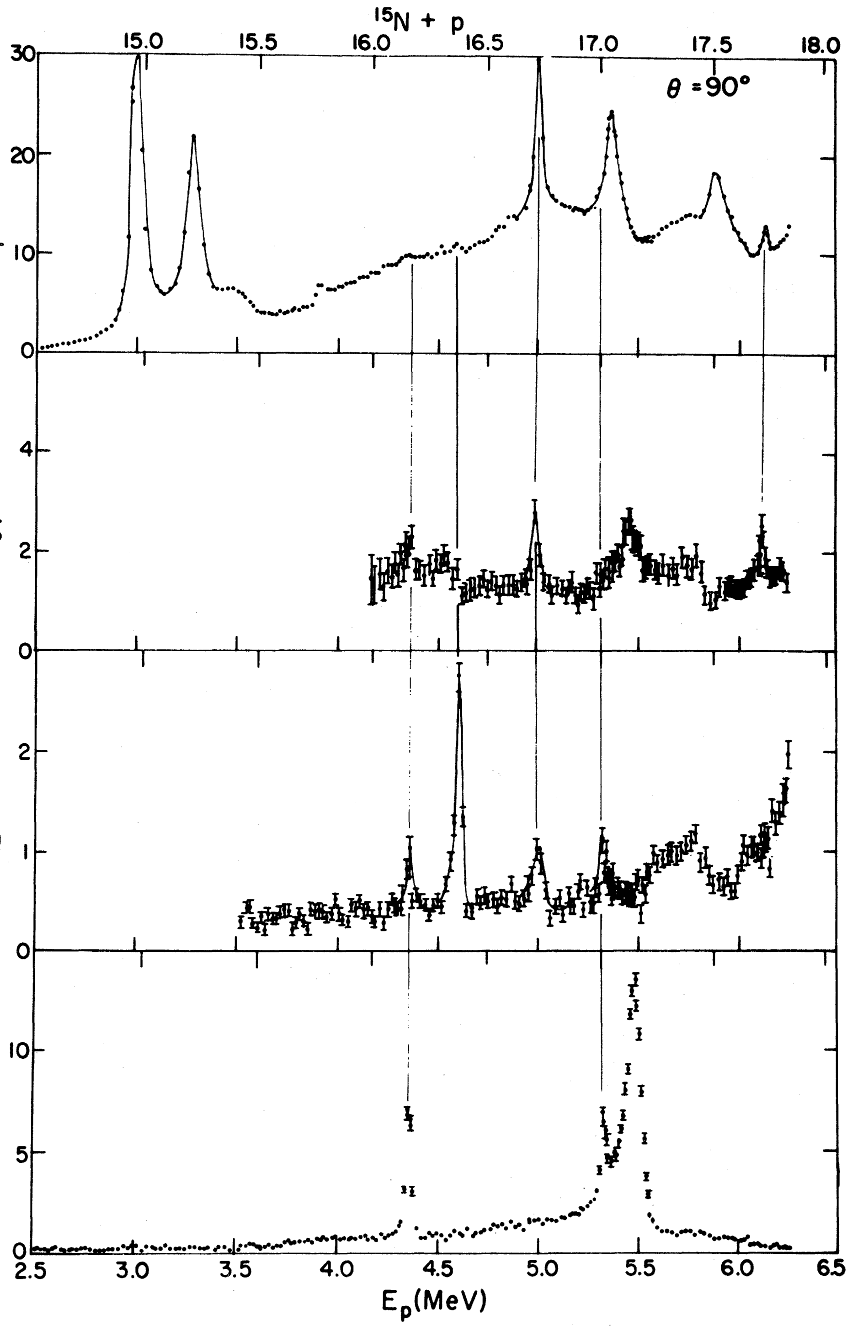

FIG. 4. Excitation functions of the γ rays from $^{15}N+p$ at energies below 6.2 MeV. Cross sections labeled $\sigma(\alpha_1\gamma)$ include contributions from the $^{12}C(p,p_1\gamma)$ reaction.

known spin we never see resonances in the cross sections which correspond to gamma decays with multipole order greater than one. Isospin assignments are based in part on the recommended upper limits (RUL's) given in Ref. 9 for $A=6$–20 isoscalar dipole decays: 0.003 W.u. for $E1$ and 0.030 W.u. for $M1$. We use the standard definition of dipole Weisskopf units, along with the relation

$$B(M1)\ (\mu_N{}^2)=1.79B(M1)\ (\text{W.u.})$$

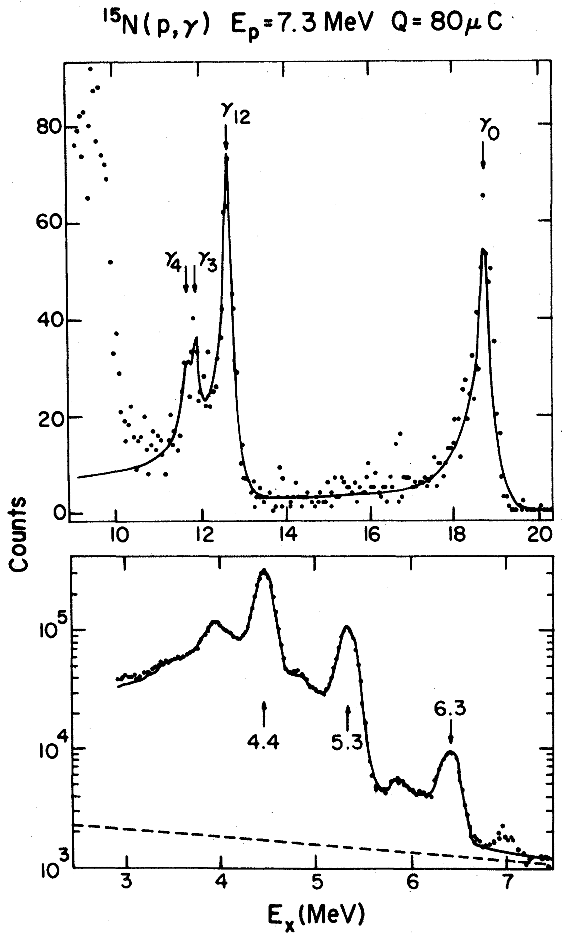

FIG. 5. Typical spectra obtained with a melamine target. The solid lines are the result of a line shape fit used in the area extraction.

between the reduced $M1$ strength in Weisskopf units and in nuclear magnetons squared.

Tentative identification of possible analog states is based in part on assuming 12.857 MeV for the average Coulomb displacement energy between ^{16}O and ^{16}N and upon similarities in the total widths of the corresponding states.

B. The $M1$ γ decay of the 16.21 and 17.12 MeV 1^+ states

The most interesting feature of the excitation functions shown in Fig. 4 is the γ_{12} decay of the 1^+ states at 16.21 and 17.12 MeV (Ref. 3). Excitation functions at $\theta=90°$ over these two resonances in ~ 5 keV steps are shown in Fig. 6. Angular distributions on and off the resonances were measured to determine the resonant Legendre coefficients. We show below that the γ_{12} resonance yields are due to γ_1. The even Legendre coefficients for the resonance γ_0 and γ_1 decays must be identical since both final states have spin zero. Hence the γ_1/γ_0 branching ratios may be determined from the 90° data alone. Our γ_{12} resonance angular distributions are consistent with the γ_0 resonance angular distributions, but the errors are quite large ($a_2 \sim -0.5\pm0.3$ and $+0.2\pm0.3$ for the 16.21 and 17.12 MeV resonances, respectively). In extracting the resonance strengths we used the a_2 coefficient determined from the γ_0 data. The present data combined with those of Ref. 3 result in improved values for these a_2 coefficients: -0.761 ± 0.061 and $+0.30\pm0.10$ for the 16.21 MeV and 17.12 MeV resonances, respectively. From the resonance areas of Fig. 6 we obtain

$$\Gamma_p\Gamma_{\gamma_0}/\Gamma=2.77\pm0.34 \text{ eV}$$

and

$$\Gamma_p\Gamma_{\gamma_1}/\Gamma=0.33\pm0.05 \text{ eV}$$

for the 16.21 MeV state and

$$\Gamma_p\Gamma_{\gamma_0}/\Gamma=4.12\pm0.58 \text{ eV}$$

and

$$\Gamma_p\Gamma_{\gamma_1}/\Gamma=0.60\pm0.08 \text{ eV}$$

for the 17.12 MeV state. These transitions labeled γ_1 could in principle be an unresolved mixture of $M1$ decay strength to the 0_2^+ (6.05 MeV) state and

TABLE I. Calculated a_2 coefficients for dipole decays.

l_1,	j_1	l_2,	j_2	J_i^π	J_f^π	a_2 (min)	a_2 (max)	a_2^{a}
1,	3/2	3,	5/2	2^+	3^-	−0.143	−0.0715	−0.107±0.036
3,	5/2	3,	7/2	3^+	3^-	0.375	0.500	0.438±0.063
3,	5/2	3,	7/2	3^+	2^+	−0.400	−0.300	−0.350±0.050
0,	1/2	2,	3/2	1^-	2^+	−0.100	0.050	−0.025±0.075
2,	3/2	2,	5/2	2^-	1^-	−0.500	−0.250	−0.375±0.125
2,	5/2	4,	7/2	3^-	3^-	0.375	0.500	0.438±0.065
2,	5/2	4,	7/2	3^-	2^+	−0.400	−0.300	−0.350±0.050

[a]Used in estimating resonance strengths in cases where angular distributions have not been measured.

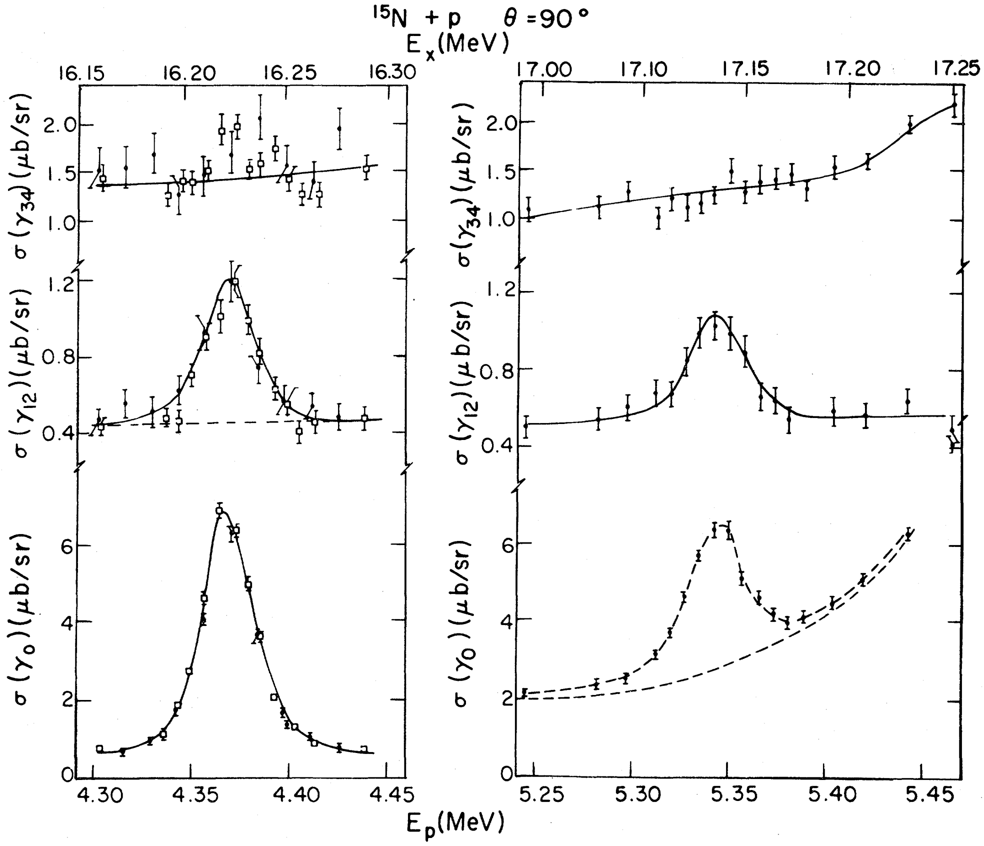

FIG. 6. Excitation functions in the vicinity of the 16.21 and 17.12 MeV states.

TABLE II. Properties of known 1^+, 1 levels in ^{16}O.

E_x (MeV) (±keV)	16.21(10)	17.12(10)	18.8(100)[a]
E_p (MeV) (±keV)	4.358(10)	5.328(10)	7.1(100)
$\Gamma_p\Gamma_{\gamma_0}/\Gamma$ (±eV)	2.77(0.34)	4.12(0.58)	≥1.8±0.3
	2.65(0.22)[a]	3.75(0.50)[a]	
	2.70(0.25)[b]	3.90(0.50)[b]	
$\Gamma_{\gamma_1}/\Gamma_{\gamma_0}$	0.119(0.007)	0.149(0.011)	
$\Gamma_{\gamma_{34}}/\Gamma^{c}_{\gamma_0}$	$0.10^{+0.05}_{-0.10}$	<0.6	
Γ_p/Γ^{d}	0.73	0.58	≤0.5
Γ (keV)	17(10)	25(8)	
	18(3)[e]	36(5)[e]	
$\Gamma^{f}_{\gamma_0}$	3.70(0.5) eV	6.72(1.0) eV	≥3.6 eV
	0.041(0.006) W.u. *M*1	0.064(0.009) W.u. *M*1	≥0.026 W.u. *M*1
$\Gamma^{f}_{\gamma_1}$	0.44(0.06) eV	1.00(0.17) eV	
	0.020(0.003) W.u. *M*1	0.035(0.006) W.u. *M*1	
$\Gamma_{\gamma_{34}}$	$0.27^{+0.13}_{-0.27}$ eV	<0.40 eV	

[a]Reference 3.
[b]Average of Ref. 3 and present results.
[c]Assumes $a_2=0$ for γ_{34}.
[d]Rough estimates from Ref. 27.
[e]Reference 11.
[f]Errors quoted neglect the uncertainty in Γ_p/Γ.

$M2/E3$ strength to the 3^- (6.13 MeV) state. However, the observed decay strengths, if all to the 3^- state, would correspond to 40—70 $M2$ Weisskopf units. Since 1 W.u. of $M2$ strength would be a very strong transition, it is clear that these decays are essentially all $M1(\gamma_1)$ with negligible $M2$ contributions. From the 90° cross sections, we get

$$\Gamma_{\gamma_1}/\Gamma_{\gamma_0}=0.119\pm0.007$$

corresponding to a ratio of

$$B(M1,\gamma_1)/B(M1,\gamma_0)=0.48\pm0.03$$

for the 16.21 MeV state. The same ratios for the 17.12 MeV state are 0.149±0.011 and 0.55±0.04, respectively. Thus the ratio of reduced strengths of the decay to the 0_2^+ state relative to the decay to the ground state is approximately the same for the 16.21 and 17.12 MeV resonances. In our data the resonance corresponding to the 17.12 MeV state has an observed width of 34 keV. Correcting for the energy loss in the target we obtain $\Gamma_{\text{c.m.}}=25\pm8$ keV, which is in fair agreement with the previously measured[10] value of 36±5 keV. The observed width of the 16.12 MeV state is 32 keV, which yields $\Gamma_{\text{c.m.}}=17\pm10$ keV. The results for the 1^+ resonances are summarized in Table II, including information from other experiments.[11]

The 1^+; $1\to0^+$; 0 ground-state $B(M1)$ values for the 16.21, 17.12, and 18.8 MeV levels of 0.075±0.010, 0.0116±0.017, and ≥0.047 (in units of $\mu_N{}^2$) are in good agreement with recent electron scattering results.[12] These electron scattering results suggest additional broadly distributed $M1$ strength in the region $E_x=17.4$ to 18.0 MeV of magnitude comparable to that of the 17.12 MeV decay strength. A substantial ground-state radiative width reported[13] for a J^π; $T=1^+$; 0 state at $E_x=13.67$ MeV has been shown[14] to be incorrect (Ref. 14 obtains $\Gamma_{\gamma_0}<1$ eV for this state).

C. The $E_x=18.98$ 4^- $T=1$ state

We observe a narrow resonance at

$$E_p=7.314\pm0.010 \text{ MeV}$$

$$(E_x=18.983\pm0.010 \text{ MeV}) .$$

The strong resonance effect in the p_{12} channel and the weak effect in the α_1 channel are consistent with the decay branches measured[15] for the 4^- $T=1$ state at

$$E_x=18.975\pm0.010 \text{ MeV}$$

strongly populated in the ^{17}O(d,t) reaction.[16] The 4^- assignment[15] was substantiated in high energy inelastic-proton scattering.[17] The inelastic scattering of π^+ and π^- revealed[18] a significant (~1% intensity) isospin mixing between this state and the neighboring 4^- $T=0$ states at $E_x=17.79$ and 19.80 MeV. In Ref. 4, it was shown from γ-γ coincidence measurements that this resonance γ decays predominantly to the 3^- (6.13 MeV) level. For the γ_2 decay of this resonance we observe $a_2=-0.28\pm0.11$, and a_1,a_3, and a_4 consistent with zero (see Table III and Fig. 7). For pure dipole decay to the 3^- level, $-0.357<a_2<-0.304$ for J(resonance)=4, $0.375<a_2<0.50$ for J(resonance)=3, and $-0.143<a_2<-0.072$ for J(resonance)=2. Hence our measured a_2 rules out $J=3$, and favors a $J=4$ assignment. Although the presence of a small $E2$ amplitude in this decay would invalidate this argument, the 4^- assignment is likely based on the other experiments discussed above. Assuming $J^\pi=4^-$, our measured a_2 leads to an amplitude mixing ratio $|E2/M1|<10\%$. A total width of 8±4 keV was determined by combining our measurement of $\Gamma_p\Gamma_{p_{12}}/\Gamma$ (neglecting interference effects) with the branching ratios of Ref. 15. The absolute widths for the various decay branches are listed in Table IV. The observed width of the 4^- state for our melam-

TABLE III. Angular distribution coefficients for the 18.03 MeV 3^-, 1 and 18.98 MeV 4^-, 1 resonances.

Channel	18.03 MeV resonance[a] a_2	18.03 MeV resonance[a] a_4	18.98 MeV resonance a_2	18.98 MeV resonance a_4
γ_{12}	0.55±0.06	0.0	−0.28±0.11	0.0
p_{12}	0.68±0.02	0.18±0.02	0.54±0.01	−0.26±0.01
α_1	−0.052±0.046[b]	0.47±0.05[b]		

[a]For the γ_{12} channel, a nonzero value of $a_1=+0.21\pm0.04$ is observed after subtracting background.
[b]These values cannot arise from an isolated 3^- resonance and hence may contain significant resonance-background interference contributions.

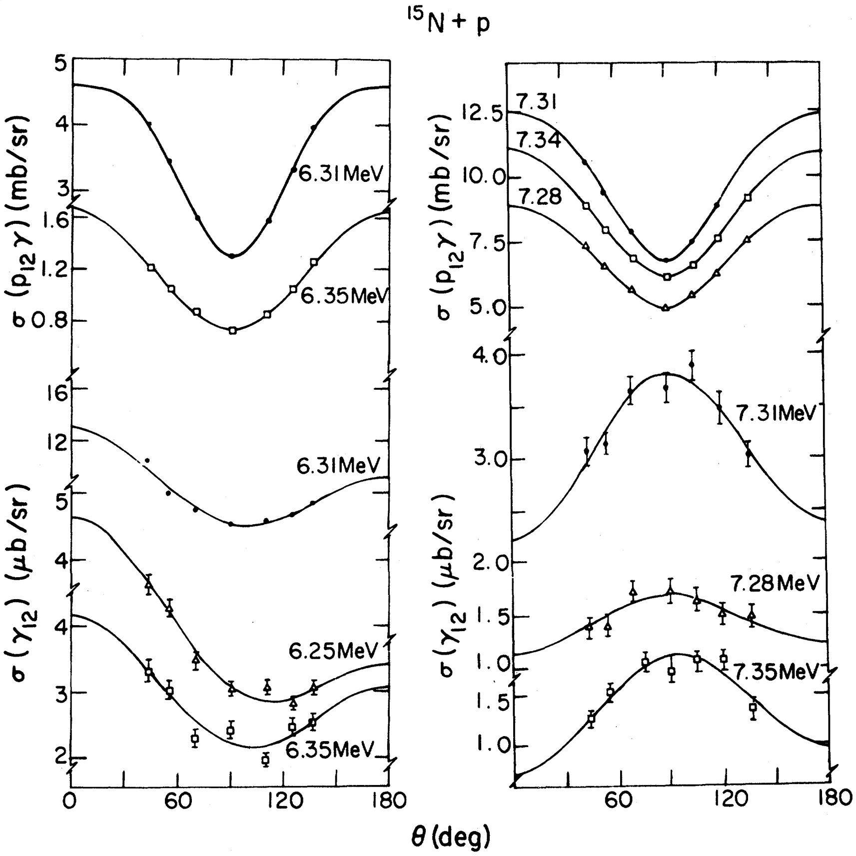

FIG. 7. Angular distributions for the $^{15}N(p,\gamma_{12})$ and $^{15}N(p,p_{12}\gamma)$ cross section in the vicinity of the 18.03 and 18.98 MeV states. The data close to 18.98 MeV were taken with a gas target, the rest with a melamine target.

TABLE IV. Properties of the $4^-;1$ and $3^-;1$ states. Results are from the present work except where noted.

$J^\pi;T$	E_p (MeV) ($\pm$keV)	E_x (MeV) ($\pm$keV)	Γ (keV)	$\Gamma_p\Gamma_x/\Gamma$	$\Gamma_{p_{12}}/\Gamma_{\alpha_1}$	Γ_x/Γ[a]	Γ_x[b]
$4^-;1$	7.314(10)	18.983(10)	8.2(3.8)[b]	0.85(0.010) eV γ_2	>7	0.12(0.05) p_0	7.1(3.1) eV γ_2
							0.16(0.07) W.u. $M1$ (γ_2)
		18.975(10)[a]		<0.03 eV γ_{34}	9(6.5)[a]	0.63(0.08) p_{12}	<0.3 eV γ_3
		18.979(7)[b]		0.618(0.086) keV p_{12}		0.02(0.05) α_0	0.98(0.19) keV p_0
				<0.09 keV α_1		0.07(0.05) α_1	5.2(2.3) keV p_{12}
							0.57(0.49) keV α_1
$3^-;1$	6.298(10)	18.032(10)	16(8)	1.96(0.27) eV γ_2	0.26(0.09)	0.41(0.15) p_0	4.8(1.9) eV γ_2
							0.14(0.06) W.u. $M1$ (γ_2)
		18.033(10)[a]	18(7)[b]	0.31(0.11) eV γ_{34}		0.02(0.05) α_0	0.76(0.39) eV γ_3
							0.026(0.013) W.u. $E1$ (γ_3)
		18.033(7)[b]		1.11(0.26) keV p_{12}		0.46(0.15) α_1	7.8(2.8) keV p_0
				4.25(1.00) keV α_1		0.11(0.15) n_0	2.7(1.2) keV p_{12}
							8.9(3.2) keV α_1

[a]Reference 16.

[b]From combining the present results with those of Ref. 16.

ine target data was 22 keV which, together with the total width given above, determines the energy loss in the target to be 20 ± 3 keV at $E_p=7.31$ MeV. Our resonance strength

$$\Gamma_p\Gamma_{\gamma_2}/\Gamma=0.85\pm0.10 \text{ eV}$$

is in agreement with a previous limit[5] of <1 eV. Using

$$\Gamma_p/\Gamma=0.12\pm0.05$$

(Ref. 15), we deduce

$$\Gamma_{\gamma_2}=7.1\pm3.1 \text{ eV} ,$$

or 0.16 ± 0.07 W.u. (see Table IV).

A particularly interesting question is the degree of purity of the dominant $(d_{5/2},p_{3/2}{}^{-1})$ configuration in the 4^-; 1 level. The p_0 entrance channel requires tiny ($<1\%$) (Ref. 15) admixtures of $(g_{9/2},p_{1/2}{}^{-1})$ configurations. The 4^-; 1 level gets most of the expected (d,t) pickup strength,[16] but only roughly one-half of the expected $M4$ inelastic electron scattering strength.[19] Our measured γ-decay strength is 0.7 ± 0.3 of the value expected for a pure $(d_{5/2},p_{3/2}{}^{-1})4^-$; 1 level (see Table VIII). Unfortunately the uncertainty in this quantity is too large to draw any interesting conclusions. This stems mostly from the large ($\pm40\%$) uncertainty in Γ_{p_0}/Γ, which should be remeasured (for example, by elastic scattering).

It is surprising that the 4^- resonance does not show sizable interference effects (see Fig. 2), as one might expect for an $M1$ resonance interfering with an $E1$ background. However, such interference would vanish due to angular momentum coupling constraints if the $E1$ background were mainly due to p-wave capture, since the 4^- resonance must be formed by g-wave capture. Alternatively, if the $E1$ background were due to a mixture of p-, f-, and h-wave capture, several interference terms would result. These could sum destructively and also lead to the very small observed interference. The possibility that the background is predominantly $M1$ can be excluded on the basis of its strength.

D. The 18.03 3^- $T=1$ state

Our resonance at

$$E_p=6.298\pm0.010 \text{ MeV}$$

$$(E_x=18.032\pm0.010 \text{ MeV})$$

occurs at the same energy as the

$$E_x=18.033\pm0.010 \text{ MeV}$$

3^- level of Ref. 15. For the γ_{12} decay of this resonance we obtain $a_2=+0.55\pm0.06$, $a_1=+0.21$ ±0.04, and a_3, a_4 consistent with zero. This is consistent with dipole decay. Assuming pure dipole decay to the 3^- 6.13 MeV level,[4] the a_2 coefficient restricts the spin of the 18.03 MeV state to $J=3$ (for which $+0.375<a_2<+0.50$), in agreement with Ref. 4. The nonvanishing a_1 indicates interference of opposite parity radiations, which suggests negative parity, since the background must be mostly $E1$. The suggestion of interference effects in $A_y(90°)$ (see Fig. 3) is also consistent with the negative parity of the state. Breuer *et al.*[15] measured $\Gamma_{p_0}/\Gamma=0.41$ and $\Gamma_{\alpha_1}/\Gamma=0.46$ [$\pm$(0.010–0.020)] for the p_0 and α_1 decays of this state. They assigned the missing strength (see Table IV) to the n_0 channel. The strong resonance we observe in the α_1 channel is consistent with the p_0 and α_1 branching ratios of Ref. 15. Our observation of a resonance in the p_{12} channel indicates that the missing 11% decay strength attributed to the neutron channel in Ref. 15 is due to the p_{12} channel. Therefore we identify this resonance as the same level populated in single-nucleon pickup studies.[15,16] The strongest evidence for the parity of this state comes from the $^{17}O(d,t)$ work[16] which reports a clear $l=1$ angular distribution shape in the region of the first maximum, implying $\pi=-$ and hence $J^\pi=3^-$. The measured a_2 given above suggests the presence of both $d_{5/2}$ and $g_{7/2}$ entrance channels, with the ratio of $g_{7/2}$ to $d_{5/2}$ amplitudes between 0.1 and 2.4.

Our measured strength

$$\Gamma_p\Gamma_{\gamma_2}/\Gamma=1.96\pm0.27 \text{ eV}$$

agrees with the less precise previous result[5] of 1.5 ± 0.8 eV. Using

$$\Gamma_p/\Gamma=0.41\pm0.15$$

(Ref. 15) we deduce $\Gamma_{\gamma_2}=4.8\pm1.9$ eV or 0.14 ± 0.06 W.u. ($M1$) (see Table IV). The results for the 18.98 and 18.03 MeV states are summarized in Tables III and IV. It is interesting to note that the 18.03 MeV 3^-;1 state theoretically does not have a strong 1p-1h component[20]; nevertheless, its $M1$ decay strength to the 3^-;0 state is as large as the decay strength of the 18.98 MeV 4^-;1 state to the same final state.

We see no evidence of the 4^- $T=0$ levels at 17.79 and 19.80 MeV which have been observed in the $^{17}O(d,t)^{16}O$ reaction[15,16] and in inelastic proton[18] and pion[19] scattering. The resonances should occur at proton energies of 6.04 and 8.18 MeV, respectively. From our data we estimate $\Gamma_{\gamma_2}<2.2$ eV (0.066 W.u.) for the 17.79 MeV state and $\Gamma_{\gamma_2}<13$ eV (0.24 W.u.) for the 19.80 MeV state. This is consistent with the rather weak p_0 decay branches of these states ($\Gamma_p/\Gamma=0.14\pm0.05$ and 0.08 ± 0.05, respectively[15]) along with their predominantly $T=0$ character,[19] which would lead to weak $M1$ decays according to Morpurgo's rule.

E. The 16.45 MeV 2^+ state

At

$$E_p=4.610\pm0.010 \text{ MeV}$$

$$(E_x=16.450\pm0.010 \text{ MeV})$$

a strong narrow resonance ($\Gamma=24\pm8$ keV) is present in the γ_{12} yield curve and absent from all other channels (see Fig. 4). We identify this resonance as a well-known 2^+ state in ^{16}O.[11] In inelastic electron scattering[10,11,21] a narrow 2^+ state was seen at $E_x=(16.46\pm0.07)$ MeV with $\Gamma=35\pm5$ keV and $\Gamma_{\gamma_0}=0.5\pm0.2$ eV. It has also been observed as a weak resonance in the $\gamma_0,\alpha_0,\alpha_1,p_0$, and n_0 exit channels in both $^{12}C+\alpha$ and $^{15}N+p$ reactions.[11] We obtain

$$\Gamma_p\Gamma_{\gamma_2}/\Gamma=1.11\pm0.24 \text{ eV}$$

assuming $J=2$ and $a_2=-0.11$ (see Table I) for the $E1$ decay to the 3^- 6.13 MeV state. From our γ_0 yields we estimate $\Gamma_p\Gamma_{\gamma_0}/\Gamma<0.21$ eV. This combined with Γ_{γ_0} from electron scattering yields $\Gamma_p/\Gamma<0.7$. $^{12}C(\alpha,\alpha)^{12}C$ and $^{12}C(\alpha,p_0)$ results[22] show a $J^\pi;T=2^+;(1)$ resonance at $E_x=16.442(2)$ MeV with $\Gamma=22\pm3$ keV, $\Gamma_{\alpha_0}/\Gamma=0.28$, and $\Gamma_{p_0}/\Gamma\simeq0.1$. Combined with our γ_2 capture strength, this yields $\Gamma_{\gamma_2}\simeq11$ eV$=0.02$ W.u.($E1$). This exceeds the RUL of 0.003 W.u. for isoscalar $E1$ transitions; hence, we assign $T=1$ to this resonance, in agreement with previous suggestions. The $^{12}C(\alpha,\gamma_0)^{16}O$ reaction strength

$$\Gamma_\alpha\Gamma_{\gamma_0}/\Gamma=0.45\pm0.11 \text{ eV}$$

(Ref. 23) together with the α_0 branching ratio quoted above leads to $\Gamma_{\gamma_0}\simeq1.6$ eV for the ground state $E2$ transition, a value considerably larger than the electron scattering result of 0.5 ± 0.2 eV.[11] The (α,γ) result may include contributions from broad $E2$ strength in this same energy region. The energy of this resonance agrees well with the expected energy of the analog in ^{16}O of the ^{16}N 3.52 MeV 2^+ state.

F. The 16.81 MeV 3^+ state

At

$$E_p=5.000\pm0.010 \text{ MeV}$$

$$(E_x=16.815\pm0.010 \text{ MeV})$$

we observe a strong, narrow resonance ($\Gamma=32\pm8$ keV) in the $\alpha_1\gamma,\gamma_{12}$, and γ_{34} yield curves. A decomposition of the γ_{34} yield indicates that the resonance is mainly due to the γ_3 decay to the 6.92 MeV 2^+ state. Assuming dipole decays limits J to 1, 2, or 3. Absence of a γ_0 transition suggests $J=2$ or 3. A 3^+ resonance has been observed at $E_p=5.01$ MeV in the $^{15}N(p,\alpha_1)$ and $^{15}N(p,p_0)$ reactions.[24] The absence of a corresponding $^{15}N(p,n_0)$ resonance[25] supports the $l=3$ assignment for this resonance since the ratio of penetrabilities $P_n/P_p=0.038$ for $l=3$, whereas $P_n/P_p=0.45$ for $l=1$. This resonance probably corresponds to the 16.80 ± 0.10 MeV (3^+) state observed[21] in inelastic electron scattering with $\Gamma<100$ keV. The analog of the 3.96 MeV 3^+ state[26] of ^{16}N is expected to occur in ^{16}O very near this resonance. For $\Gamma_p/\Gamma=0.5$ (see Table V) the $M1$ transition strength somewhat exceeds the RUL for an isoscalar transition. Thus we suggest $T=1$ for the resonance. However, our $(p,\alpha_1\gamma)$ strength implies $\Gamma_{\alpha_1}\approx14$ keV (see Table V), indicating significant isospin mixing.

G. The 17.27 MeV 1^- $T=1$ state

The resonance in the γ_{34} channel at

$$E_p=5.488\pm0.015 \text{ MeV}$$

$$(E_x=17.27\pm0.015 \text{ MeV})$$

corresponds to the decay of the well-known[11] 17.29 $J=1^-$, $T=1$ state. Analysis of our gamma ray spectra indicates that the γ_{34} resonance is an $E1$-decay branch to the 2^+ 6.92 MeV state of ^{16}O. Assuming $a_2=-0.025$ (see Table I) we obtain

$$\Gamma_p\Gamma_{\gamma_3}/\Gamma=3.27\pm0.41 \text{ eV}$$

for this branch. Resonance analysis of the γ_0 data of Ref. 3 constrained to reproduce cross sections and analyzing powers at 90° as well as the a and b coefficients over an extended energy region yields

$$\Gamma_p\Gamma_{\gamma_0}/\Gamma=(25\pm6) \text{ eV},$$

in agreement with an estimate of this strength based on the present data. Using[11,27] $\Gamma_p/\Gamma=0.41$ we obtain $\Gamma_{\gamma_0}=61$ eV, in good agreement with previous radiative capture results[11] ($\Gamma_{\gamma_0}=67$ eV) and inelastic electron scattering results[11,21] ($\Gamma_{\gamma_0}=62\pm12$ eV). We estimate

$$\Gamma_{\gamma_3}/\Gamma_{\gamma_0}=0.134\pm0.025$$

for this state, which yields $\Gamma_{\gamma_3}=8$ eV or 0.015 W.u. ($E1$).

TABLE V. Additional ^{15}N + p resonances which produce gamma rays. Results are from the present work except where noted.

E_p (MeV) (±keV)	E_x (MeV) (±keV)	$J^\pi;T$	$J^\pi;T$ assumed	$\Gamma_{c.m.}$ (keV) (±keV)	$\Gamma_p\Gamma_{\gamma_2}/\Gamma$ (eV) (±eV)	$\Gamma_p\Gamma_{\gamma_{34}}/\Gamma$ (eV) (±eV)	$\Gamma_p\Gamma_x/\Gamma$ (keV)[a]	Γ_p/Γ	Γ_{γ_2}	$\Gamma_{\gamma_{34}}$
2.995(15)	14.936(15)		$2^+;0$	53(8)			16.4 (α_1)	0.48[b]		
	14.922(6)[b]	2^+[b]		65(5)[b]						
3.288(15)	15.210(15)		$2^-;0$	64(8)			10.9 (α_1)	0.8[b,c]		
	15.196(3)[b]	2^-[b]		58(10)[b]						
4.610(10)	16.450(10)	1–4[d]	$2^+;1$	24(8)	1.11(0.24)			≃0.1[e]	≃11 eV 0.02 W.u. $E1$	
	16.442(2)[b]	$2^+;(1)$[b]		22(3)[b]						
5.000(10)	16.815(10)	1,2,3[d]	$3^+;1$	32(8)	0.48(0.09)	0.62(0.13) γ_3	6.8 (α_1)	0.5[f]	1.0 eV 0.002 W.u. $E1$	1.2 eV (γ_3) 0.06 W.u. $M1$ (γ_3)
	16.817(2)[b]	3^+[b]		70(10)[b]						
5.488(15)	17.271(15)[g]	1^-	$1^-;1$	77(10)[g]		3.27(0.41) γ_3		0.41[b]		8 eV (γ_4) 0.017 W.u. $E1$ (γ_3)
	17.27(20)	$1^-;1$[b]		90(10)						
6.138(10)	17.880(10)	0,1,2[d]	$2^-;1$	19(8)		0.69(0.10) γ_4	1.48 (α_1)	0.35[f]		2 eV (γ_4) 0.08 W.u. $M1$ (γ_4)
	17.6(100)[h]	2^-[h]		< 100[h]						
8.288(10)	19.896(10)	1–4	$3^{(+)};1$	38(10)	3.91(0.56)		1.07 (α_1) 4.48 (p_{12}) 0.52 (p_3)	0.35[f]	11 eV 0.010 W.u. $E1$	
	19.90(20)[i]	3[i]		75(30)[i]	~5[i]					
8.836(20)	20.412(20)	1–4	$4^+;1$[j]	190(20)	18.8(3.9)		15.8 (p_{12}) 5.8 (p_3) 22 (n_0)[k]	0.5[f]	38 eV 0.030 W.u. $E1$	
	20.43(30)[i]	2,4[i]		190(40)[i]	54(20)[i]					

[a]Inferred from reaction γ-ray yields (uncertainty ±20%).
[b]Reference 11.
[c]Reference 15.
[d]Assuming dipole γ decays.
[e]Reference 22.
[f]See Sec. IV A.
[g]From a resonance analysis of the γ_0 data of Ref. 3 (see Sec. IV G).
[h]Reference 21.
[i]Reference 5.
[j]We believe the previous 2^- assignment (Refs. 5 and 11) to be incorrect (see Sec. IV H).
[k]From Ref. 30, corrected for $J=4$.

H. Other resonances

The strong resonances (see Fig. 4) observed in the $\alpha_1\gamma$ yield curve at $E_p=2.995(15)$ and 3.288(15) MeV [$E_x=14.936(15)$ and 15.210(15) MeV, respectively] correspond to well established states[11] in ^{16}O at excitation energies of 14.922(6) and 15.196(3) MeV with assigned spins of 2^+ and 2^-, respectively. The 2^+ resonance has

$$\Gamma_p\Gamma_{\alpha_1}/\Gamma^2=0.31\pm0.08$$

(see Table V), indicating nearly equal p_0 and α_1 widths (and consequently a very small α_0 width), consistent with Ref. 11. Breuer *et al.*[15] observed the population and decay of the 2^- resonance in the ^{17}O(d,tc) reaction with $c=p_0$ and α_1, and found $\Gamma_{p_1}/\Gamma=0.81$ and $\Gamma_{\alpha_1}/\Gamma=0.19$; hence, $\Gamma_p\Gamma_{\alpha_1}/\Gamma^2 \simeq 0.15$, consistent with our result of 0.17 ± 0.14.

Near $E_p=3.47$ MeV ($E_x=15.38$ MeV) we observe a broad peak in the $\alpha_1\gamma$ channel with $\Gamma=200$ keV which is not resolved from the strong resonance in this channel at $E_p=3.29$ MeV. This peak does not agree with any single known resonance in ^{16}O.

The broad structure around $E_p=5.7$ MeV in the γ_{12} and α_1 yield curves suggests the presence of resonances at $E_x=17.40$ and 17.55 MeV, both with widths of roughly 150 keV.

The relatively strong resonances in the 4.4 MeV γ-ray yield curve at $E_p=5.375$ and $E_p=5.89$ MeV agree with known resonances in the ^{12}C(p,p_1)^{12}C*(4.43) reaction.[8] We ascribe these resonances to the ^{12}C($p,p_1\gamma$4.43) reaction on the carbon contained in the melamine target.

At

$$E_p=6.138\pm0.010 \text{ MeV}$$

$$(E_x=17.880\pm0.010 \text{ MeV})$$

we observe a narrow resonance ($\Gamma=10\pm8$ keV) in the γ_{34} and α_1 channels (see Fig. 4). A decomposition of the γ_{34} yield indicates that the resonance is due to γ_4, which populates the 1^- 7.12 MeV final state. Thus we expect $J=0$, 1, or 2 for the resonance. It is possible that this resonance corresponds to the (2^-) state seen in inelastic electron scattering[21] at 17.6 ± 0.1 MeV with $\Gamma<100$ keV. The analog of the 5.05 MeV 2^- level[11] in ^{16}N is expected about 17.88 MeV (see Table VI), suggesting a (2^-,1) assignment for our resonance, an $M1$ decay to the 7.12 1^- state, and an isospin mixed character for the resonance.

Relatively weak overlapping resonances are apparent in $\alpha_1\gamma$, $p_{12}\gamma$, and $p_3\gamma$ at

$$E_p=7.54\pm0.05 \text{ MeV}$$

$$(E_x=19.20\pm0.05 \text{ MeV})$$

and

$$E_p=7.86\pm0.05 \text{ MeV}$$

$$(E_x=19.50\pm0.05 \text{ MeV})$$

and in $\alpha_1\gamma$, $p_{12}\gamma$, and γ_{12} at

$$E_p=7.65\pm0.05 \text{ MeV}$$

$$(E_x=19.30\pm0.05 \text{ MeV}),$$

TABLE VI. Some probable analog $T=1$ states in ^{16}O and ^{16}N.

^{16}N[a]			^{16}O[b]			
E_x (MeV) ($\pm$keV)	Γ (keV)	J^π	E_x (MeV) ($\pm$keV)	Γ (keV)	J^π	E_N-E_0 + 12857 keV
3.355(5)	15(5)	1^+	16.212(10)	18(3)[a]	1^+	0(11)
3.519(5)	3	2^+	16.442(2)[a]	24(8)	2^+	−66(5)
3.960(5)	≤2	3^+	16.817(2)[a]	32(8)	3^+	0(5)
4.319(5)	20(5)	1^+	17.123(10)	36(5)[a]	1^+	53(11)
4.387(6)	82(20)	1^-	17.271(15)	77(10)	1^-	−27(16)
4.760(50)	250(50)	1^-	~17.5[c]	~500[c]	1^-	
4.776(10)	59(8)	2^+	17.72[a]	~75[a]	(0^+,2^+)[a]	−87
5.050(16)	19(6)	2^-	17.880(10)	19(8)	(2^-)	27(18)
5.150(7)	≤11	$(2,3)^-$	18.033(7)	16(8)	3^-	−26(10)
6.009(10)	270(30)	1^-	18.990(30)[a]	260[a]	1^-	−124(31)
6.168(4)	≤11	(4^-)	18.979(7)	8(4)	4^-	46(8)
6.426(7)	300(30)		19.48(25)[a]	250(50)	1^-	−197(26)

[a]Reference 11.
[b]This work unless otherwise noted.
[c]Visible in data of Ref. 6.

with widths $\sim$130–200 keV. The lower resonance occurs at the same energy as the 3^- $T=1$ state seen by Breuer *et al.*[15] with $\Gamma=68\pm10$ keV, but is considerably broader.

The

$$E_p=8.288\pm0.010 \text{ MeV}$$

$$(E_x=19.896\pm0.010 \text{ MeV})$$

resonance was studied previously by Chew *et al.*,[4,5] who showed that the γ_{12} decay is to the 3^- (6.13 MeV) final state and assigned $J=3$ to the resonance. There is also some evidence of a narrow ($l=3$) resonance at this energy in the ^{15}N(p,p) excitation functions of Dearnaley,[28] suggesting $\pi=+$.

Finally, at

$$E_p=8.836\pm0.020 \text{ MeV}$$

$$(E_x=20.412\pm0.020 \text{ MeV}) ,$$

we observe a very strong resonance which has previously been studied[4,5] in the ^{15}N(p,γ_2) reaction. Strong resonance-background interference was observed in the 90° γ_{12} yield, due to interference effects in the a_2 coefficient. This was interpreted as arising from $J=4$ resonance–$J=2$ background or $J=2$ resonance–$J=4$ background interference.[5] The authors of Refs. 4 and 5 argued that the 20.41 MeV state is the giant $M1$ resonance built upon the 3^- (6.13 MeV) level and suggested on the basis of the agreement in excitation energy that this is the 2^- ($M2$) resonance seen at $E_x=20.36\pm0.07$ MeV in inelastic-electron scattering. However, the resonance widths do not agree: $\Gamma=190\pm20$ keV for the (p,γ_2) resonance[5] and $\Gamma=500\pm100$ keV for the (e,e') resonance.[11,21,29] An assignment of $E1$ to the resonant γ_2 transition is more likely. The observed interference in a_2 requires interfering resonance and background amplitudes of the same parity. The predominant multipolarity in the background is almost certainly $E1$; thus, this effect is simply explained if the resonant γ_2 yield is also $E1$. If the resonance were $M1$, then a substantial portion ($\gtrsim 50\%$) of the background would have to be $M1$ ($E2$ capture could not be sufficiently strong), and one would expect large off-resonance $E1$-$M1$ interference in this region, which is not observed either in the a_1 coefficients of Ref. 5 or in our 90° analyzing power A_y (90°) for γ_2 (Fig. 1). This argues that this resonance is $E1$; hence, $J^\pi=2^+$ or 4^+. In this case $4^+(f_{7/2})$-$2^+(p_{3/2})$ interference would account for the behavior in the a_2 observed in Ref. 5. If we identify this resonance as the one seen at $E_p=8.88\pm0.04$ MeV in the (p,n) reaction,[25,30] then the observed reaction strengths (see Table V) are incompatible with $J=2$. Hence we assign $J^\pi=4^+(2^+)$, $T=1$ to this resonance. This is likely the same resonance observed[31] in $(p,p_{0,2})$ at $E_x=20.42$ MeV, which on the basis of weak evidence was tentatively assigned $J^\pi=(2^+,3^+,4^+)$. Also, elastic α scattering suggests[22] a (4^+) resonance at this energy with about the right width. A $T=1$ state with $J^\pi=(2^-,4^-)$ seen[16] at $E_x=20.45$ MeV in $l=1$ pickup from ^{17}O must correspond to a different level.

V. IDENTIFICATION OF $T=1$ ANALOG STATES IN ^{16}O AND ^{16}N

Because of the selection rules favoring $\Delta T=1$ for both $E1$ and $M1$ transitions, it is likely that the ^{15}N(p,γ) resonances we observe correspond to $T=1$ states. We have reviewed the isospin assignments for most of the resonances above. Our assignments are summarized in Table VI. In Table VI we list the excitation energies and widths of the suggested corresponding states of ^{16}N and ^{16}O along with the excitation energy difference in ^{16}N and ^{16}O normalized to zero for the lowest 1^+ $T=1$ state. It is clear from the small value of this difference, and the near equality of the corresponding level widths in ^{16}N and ^{16}O, that our assignments are reasonable. We have noted above that isospin nonconserving α decay branches are observed for most of the ^{15}N(p,γ) resonances. This does not invalidate the $T=1$ assignments because the α widths are a very small fraction of the Wigner-limit width. The α branching ratios are relatively large, not because the α widths are large, but because the proton widths are small. The smallness of the proton widths is a consequence of the 2p-2h nature of the positive parity $T=1$ states. This configuration could decay readily to the 5 MeV 1p-2h states of ^{15}N (which are energetically closed below $E_x=17.40$ MeV). On the other hand, decays to the ^{15}N ground state are strongly suppressed. Similarly the proton widths of the negative parity $E1$ states are configuration inhibited; for example, the $d_{5/2}p_{3/2}{}^{-1}$ structure of the 19.0 MeV 4^- state inhibits its decay to the ^{15}N ground state. Both the 6.01 MeV 1^- and the 6.43 MeV ^{16}N levels[11] appear to be analogs of known 1^- levels in ^{16}O (see Table VI). The parent in ^{16}N (expected near 6.0 MeV) of the broad 18.8 MeV ^{16}O $1^+;1$ level has not been identified. Most likely this ^{16}N 1^+ state is not resolved from neighboring levels such as the 6.01 MeV 1^- state. Other 1^+ states assigned in ^{16}N have no known ^{16}O analogs.[11]

VI. THEORETICAL DISCUSSION

We are primarily concerned with a comparison in ^{16}O between the present experimental gamma widths and theory. We will show that the available theoretical models have some success in explaining the data but also some serious failures, in particular for the $M1$ transitions to the 1^+ $T=1$ states. In order to illuminate the reasons for these failures, we have expanded our comparisons to include $M1$, Gamow-Teller, and (p,n) observables in the region $A=14-18$ as well as the two-nucleon transfer reactions leading to the 1^+ $T=1$ states.

Although a number of interesting collective models have been applied to the description of excited states in ^{16}O, such as the alpha cluster model[32] and the deformed Nilson model,[33] these models have thus far only been developed for the $T=0$ states. For the isovector transitions, the interplay between single-particle and collective excitations is important and we must turn to a more microscopic description as provided by the shell-model configuration mixing theory.

Since the first excited state of ^{16}O (the 6 MeV 0^+ state) is known to have a 4p-4h configuration, a "good" shell-model calculation of ^{16}O and neighboring nuclei should be one which permits up to $4\hbar\omega$ excitations out of the $0s$ and $0p$ shell cores. The basis dimensions for such a calculation are prohibitively large (there are, for example, 2337 4p-4h 0^+ states) and some truncations must be made in order to keep the number of basis states down to a manageable size. In ^{16}O two different kinds of configurations relative to a $(0s,0p)$ closed shell are known to be important for the low lying levels. Namely, the 1p-1h configurations for vibrational type of states such as the 3^- $T=0$ "octupole vibration" and the 1^- $T=1$ "giant-dipole vibration," and the many-particle-many-hole configurations for the deformed type states such as the low-lying "4p-4h" rotational band.

A single truncation which simultaneously incorporates both of these features has yet to be successfully developed. Rather, one truncation has been developed[34,35] which works best for describing vibrational collectivity and another[36–39] which works best for describing the many-particle-many-hole states. In the next section we briefly describe some recent versions of these two truncations schemes.

A. The ZBM model space

This model space restricts the active orbits to the $0p_{1/2}$, $0d_{5/2}$, and $1s_{1/2}$ subshells outside of a closed $(0s_{1/2},0p_{3/2})$ (^{12}C) core and is referred to as the "ZBM" model space after the authors instrumental in its early development.[36,37] The ZBM truncation has been very successful in giving a microscopic description of the low lying "many-particle-many-hole" holes states for nuclei around ^{16}O. The parameters of the effective interaction in this model are usually taken as the three single-particle energies and the 30 independent two-body matrix elements.

Initially, the two-body matrix elements were based on a realistic interaction, then some or all of them along with the three single-particle energies were varied to fit experimental binding energies for $A=13-18$.[36,37] More recently[38,39] two interactions have been extensively tested which are referred to as the "F" and "Z" interactions in Ref. 39. The comparisons made in Ref. 39 and the comparisons of electromagnetic matrix elements we have calculated have shown no clear preference for one interaction over the other, and most results presented here will be those for the Z interaction.

Arima and Strottmann[40] have calculated $M1$ strengths in ^{16}O using the ZBM model space with the "ZBM-II" interaction of Ref. 36. The $M1$ strength distribution with this interaction is similar to the results given here for the Z interaction. (Note that the ZBM calculations shown in the figure of Ref. 40 do not include 4p-4h components in the 0^+ and 1^+ states.)

The major deficiency of the ZBM model space is that it does not include the $0d_{3/2}$ and $0p_{3/2}$ levels. These will enter as intruder states at about 6 MeV above the nonclosed shell configurations and will modify the $M1$ observables for transitions within the ZBM model space.

B. The PSD model space

In the PSD model space the $0p_{3/2}$, $0p_{1/2}$, $0d_{5/2}$, $1s_{1/2}$, and $0d_{3/2}$ orbits are all active. Millener and Kurath (MK) (Ref. 35) have determined an effective interaction appropriate for a truncation in which the normal parity states are constrained to a major oscillator shell and the non-normal parity states are constrained to $1\hbar\omega$ excitations, e.g., $0p$ to $0d1s$ excitations. The residual interactions consist of the $0\hbar\omega$ matrix elements of the type

$$\langle 0p\text{-}0p \mid V \mid 0p\text{-}0p \rangle$$

and

$$\langle 0d\,1s\text{-}0d\,1s \mid V \mid 0d\,1s\text{-}0d\,1s \rangle ,$$

the $1\hbar\omega$ matrix elements such as

$$\langle 0p\text{-}0d\,1s \mid V \mid 0p\text{-}0d\,1s \rangle ,$$

and the $2\hbar\omega$ matrix elements such as

$$\langle 0p\text{-}0p \mid V \mid 0d\,1s\text{-}0d\,1s \rangle .$$

The total interaction which we refer to as the MK interaction consists of the following:

$0\hbar\omega$. The Cohen-Kurath "8–16-TBME" interaction[1] for the $0p$ shell; the Preedom-Wildenthal interaction[2] for the $0d\,1s$ shell.

$1\hbar\omega$. The $1\hbar\omega$ MK interaction is based on a Yukawa potential with 11 parameters for the central, *LS*, and tensor interactions. These are chosen to give a good account of the non-normal parity states of a number of nuclei from ^{11}Be to ^{16}O (Ref. 35).

$2\hbar\omega$. The Kuo-Brown G matrix.[41]

We are also interested in using the MK interactions to calculate the 2p-2h 0^+ and 1^+ states in ^{16}O which are central to understanding the $M1$ and GT decays involving the 1^+ states. To remove the spurious states the full basis must include

$$(0s)^4(0p)^{12},(0s)^4(0p)^{10}(0d\,1s)^2,(0s)^3(0p)^{12}(0d\,1s)^1$$

and

$$(0s)^4(0p)^{11}(0f\,1p)^1$$

configurations. The calculations we have carried out do not include excitations into or out of the $0s$ and $0f\,1p$ shells (the latter two components given above). However, we have compared some of our results with calculations of Millener,[20] which include all four configurations, and the differences were small.

Arima and Strottman (AS) (Ref. 40) have also carried out calculations for ^{16}O with the first two configurations above (they allow only one particle in the $0d_{3/2}$ orbit; however, we have checked that the same restriction in the present calculation does not significantly change the $M1$ matrix elements to the states of interest). The total AS interaction consists of the following:

$0\hbar\omega$. The Cohen-Kurath interaction[1] for the $0p$ shell; the Kuo-Brown G-matrix elements[42] for the $0d\,1s$ shell.

$1\hbar\omega$. The Gillet interaction.[34]

$2\hbar\omega$. The Gillet interaction.

Clearly the MK and AS interactions differ in many respects. We expect the MK interaction to be more reliable, since it has been tied more closely to experimental binding energies and excitation energies. The major deficiency of the MK-PSD model is that the energies of the many-particle-many-hole states in ^{16}O come at too high an excitation with the MK interaction.

C. The spurious state problem

With harmonic-oscillator wave functions it can be shown[43] that the closed-shell configuration for ^{16}O can be factored into a product of intrinsic and center of mass wave functions with the center of mass in a $0s$ state. There is one $1\hbar\omega$ excitation which excites the center of mass into a $0p$ state, and hence one particular linear combination of 1p-1h states for $J=1^-$ and $T=0$ will be spurious and unphysical. In *j-j* coupling this linear combination is proportional to

$$\sum_{ph} \langle ph \| \vec{R} \| 0 \rangle \, | ph \rangle \propto \sum_{ph} \langle p \| rY^{(1)} \| h \rangle \, | ph \rangle \, ,$$

where

$$\vec{R}=\frac{1}{A}\sum_i \vec{r}(i)$$

is the center of mass coordinate.

In the PSD-MK model space this spurious state can easily be eliminated, for example by using the method of Gloeckner and Lawson (GL).[44] However, since the ZBM 1p-1h spectrum is incomplete (i.e., the $0p_{3/2}$ and $0d_{3/2}$ orbits are missing) there is only one 1^- state, the $0p_{1/2}{}^{-1}1s_{1/2}{}^{1}$ configuration, and the spurious state cannot be eliminated. The two approximate extremes are to use the GL method, which has the effect of eliminating all 1^- states from the ZBM 1p-1h spectrum,[45] or to keep the wave functions unmodified. The $0p_{1/2}{}^{-1}1s_{1/2}{}^{1}$ configuration is in fact 95% nonspurious (i.e., this configuration contributes 5.4% to the above spurious wave function), and hence it is more reasonable to use the latter approximation of leaving the ZBM wave functions unmodified.

The spurious 1^- $T=0$ state is involved in the 2p-2h states of ^{16}O since spurious 2p-2h states can be made by the coupling of a nonspurious 1p-1h and the spurious 1p-1h state. In the PSD 2p-2h spectrum it is very important to remove these components, which we have done by using the GL method. In addition, the center of mass can be directly excited by $2\hbar\omega$ into $0d$ and $1s$ states which are represented by a linear combination of $2\hbar\omega$ 1p-1h and 2p-2h shell-model configurations. Our calculations do not include these $2\hbar\omega$ 1p-1h states, but comparisons with some calculations of Millener,[20] who has included $2\hbar\omega$ 1p-1h, suggest that their effects on the results presented here are small.

D. General comparison of $M1$, GT, and (p,n) observables

The reduced $M1$ and GT transition probabilities are historically defined as:

$$B(M1)=56.8\,\mu_N{}^2/[\tau\,(\mathrm{fs})E\,(\mathrm{MeV})^3]$$

$$=86.4\Gamma_\gamma(\mathrm{eV})/E\,(\mathrm{MeV})^3\, ,$$

$$B(\mathrm{GT})+B(F)=6170/[t_{1/2}(\mathrm{s})f]\, ,$$

where $B(F)$ is the reduced Fermi transition probability.

The trivial statistical dependence on J_i and J_f can be removed by defining related reduced matrix elements M by

$$M(M1)=[(2J_i+1)B(M1)]^{1/2}$$

and

$$M(\mathrm{GT})=[(2J_i+1)B(\mathrm{GT})]^{1/2} .$$

With these definitions, $M(M1)$ and $M(\mathrm{GT})$ are related to

$$M(M1)=(-1)^{T_f-T_z}\begin{bmatrix} T_f & 0 & T_i \\ -T_z & 0 & T_z \end{bmatrix}\langle f|||O(ISM1)|||i\rangle+(-1)^{T_f-T_z}\begin{bmatrix} T_f & 1 & T_i \\ -T_z & 0 & T_z \end{bmatrix}\langle f|||O(IVM1)|||i\rangle ,$$

$$M(\mathrm{GT})=(-1)^{T_f-T_{zf}}\begin{bmatrix} T_f & 1 & T_i \\ -T_{zf} & \Delta T_z & T_{zi} \end{bmatrix}\langle f|||O(\mathrm{GT})|||i\rangle .$$

The reduced matrix element convention is

$$\langle J_f,M_f\,|\,T_q^{(k)}\,|\,J_i,M_i\rangle =(-1)^{J_f-M_f}\begin{bmatrix} J_f & k & J_i \\ -M_f & q & M_i \end{bmatrix}\langle J_f||T^{(k)}||J_i\rangle .$$

The magnetic moments are proportional to matrix elements of the $O(M1)$ operators, and by definition,

$$\mu=(4\pi/3)^{1/2}\begin{bmatrix} J & 1 & J \\ -J & 0 & J \end{bmatrix}M(M1) .$$

In the impulse approximation for weak and electromagnetic interactions, in which the nucleons are treated as point particles and the nuclear recoil is ignored, $O(M1)$ and $O(\mathrm{GT})$ are given by the following one-body operators:

$$O(ISM1)/\mu_N =(3/4\pi)^{1/2}[(g_{sp}+g_{sn})\vec{s}+(g_{lp}+g_{ln})\vec{l}\,]/2 ,$$

$$O(IVM1)/\mu_N =(3/4\pi)^{1/3}[(g_{sp}-g_{sn})\vec{s}\,\vec{\tau}+(g_{lp}-g_{ln})\vec{l}\,\vec{\tau}]/2 ,$$

and

$$O(\mathrm{GT})=(g_A/g_V)(2)^{1/2}\vec{s}\,\vec{\tau} ,$$

$$\vec{s}=\Sigma\vec{s}(i) ,$$

$$\vec{l}=\Sigma\vec{l}(i) ,$$

$$\vec{s}\,\vec{\tau}=\Sigma\vec{s}(i)\vec{\tau}(i) ,$$

and

$$\vec{l}\,\vec{\tau}=\Sigma\vec{l}(i)\vec{\tau}(i) .$$

The ratio of the axial vector to vector coupling constants is determined from the neutron beta decay[46]

$$|g_A/g_V|=1.251\pm0.009 ,$$

and g_p and g_n are the free proton and neutron g factors ($g_{sp}=5.585$, $g_{sn}=-3.826$, $g_{lp}=1.$, and $g_{ln}=0.$). The "free" nucleon values may be renormalized[47] due to many-$\hbar\omega$ configuration mixing outside that contained in our model space.

Beyond the impulse approximation, processes such as the delta-particle-nucleon-hole admixtures[48] will contribute to the renormalization of the $\vec{s}\,\vec{\tau}$ operator equally for both the $M1$ and GT observables. There is presently considerable controversy as to whether this or the many-$\hbar\omega$ admixtures are more important.[49]

On the other hand, meson exchange and pair current diagrams contribute quite differently to the vector $M1$ and axial vector GT operators,[50] so that the "effective" operators for $\vec{s}\,\vec{\tau}$ may be different for $M1$ and GT observables. [Note in Eq. (5.18) of Ref. 50 that pair-current contributions are proportional to $M(\text{proton})/M(\pi)$ for the vector and $M(\pi)/M(\text{proton})$ for the axial-vector operators.]

The various isovector probes may be directly compared by relating them to the basic reduced matrix elements,

$$R(\vec{s}\,\vec{\tau})=\langle f|||\vec{s}\,\vec{\tau}|||i\rangle$$

and

$$R(\vec{l}\,\vec{\tau})=\langle f|||\vec{l}\,\vec{\tau}|||i\rangle .$$

[Note that for a free nucleon $R(\vec{s}\,\vec{\tau})=3$ and $R(\vec{l}\,\vec{\tau})=0$.] We define reduced matrix elements related to the various probes such that the leading term is equal to $R(\vec{s}\,\vec{\tau})$:

$$R(IVM1)=M(IVM1)\Bigg/\left[(3/4\pi)^{1/2}\begin{bmatrix} T_f & 1 & T_i \\ -T_z & 0 & T_z \end{bmatrix}(g_{sp}-g_{sn})/2\right]$$

$$=R(\vec{s}\,\vec{\tau})+[(g_{lp}-g_{ln})/(g_{sp}-g_{sn})]R(\vec{1}\,\vec{\tau})$$

$$=R(\vec{s}\,\vec{\tau})+0.1062R(\vec{1}\,\vec{\tau})\,,$$

$$R(\mathrm{GT})=M(\mathrm{GT})\Big/\left[(2)^{1/2}\,|g_A/g_V|\,\begin{pmatrix} T_f & 1 & T_i \\ -T_{zf} & \Delta T_z & T_{zi}\end{pmatrix}\right]=R(\vec{s}\,\vec{\tau})\,.$$

In these relations, unnecessary phase factors have been dropped.

It was recently discovered that the (p,n) reaction cross sections for medium energy protons at small angles are dominated by $L=0$ and $S=1$ transfer.[51] Hence, the small-angle cross sections are proportional to the same matrix element which mediates Gamow-Teller beta decay. The proportionality constant has been established empirically by comparing the (p,n) cross sections and B(GT) matrix elements between the same initial and final states.[52] The matrix elements $R(pn)$, which are defined in the same way as R(GT), can then be extracted for many transitions which are energetically inaccessible to beta decay. This has led to a tremendous increase in our knowledge about many individual states connected via the $\vec{s}\,\vec{\tau}$ operator as well as about the features of the "giant Gamow-Teller" resonance in general. We will define a quantity $B(pn)$ extracted from the (p,n) experiments[53–55] in such a way that it would equal B(GT) between the same two states (i.e., it contains the factor g_A/g_V).

In the following comparisons of theory and experiment we have used, in addition to the present experimental results, data obtained from the compilations[56,57] and from other works[12,58–62] not covered by the compilations.

There are many cases in the mass region $A=13-18$ where $M1$ and GT strengths connecting the same pairs of states have been measured. The experimental matrix elements M and R for a number of these are given in Table VII. (Note that the signs of M and R are only meaningful for the diagonal cases, which are related to the isovector magnetic moments.)

The theoretical matrix elements $R(\vec{s}\,\vec{\tau})$ and $R(\vec{1}\,\vec{\tau})$ are also given in Table VII for the ZBM and PSD calculations. We first discuss some general features of the comparison of experiment with theory. It is convenient to consider the experimental quantity $R(IVM1)$ with the theoretical $\vec{1}\,\vec{\tau}$ contribution subtracted,

$$\tilde{R}(IVM1)\equiv R(IVM1)\pm 0.1062R(\vec{1}\,\vec{\tau})\,.$$

For diagonal (magnetic moment) matrix elements the sign is negative, and for the off-diagonal $M1$ matrix elements the sign is determined by the relation between the theoretical $\vec{s}\,\vec{\tau}$ and $\vec{1}\,\vec{\tau}$ matrix elements.

In Table VII we compare the quantities R(GT), $\tilde{R}(IVM1)$, and $R(\vec{s}\,\vec{\tau})$ whose absolute values should be equal if experiment and theory agree. In Fig. 8, the quantities R(GT) and $\tilde{R}(IVM1)$ (ZBM) are compared in an (x,y) plot and in Fig. 9 the quantities R(GT), $\tilde{R}(IVM1)$(PSD-MK), $R(\vec{s}\,\vec{\tau})$(ZBM), and $R(\vec{s}\,\vec{\tau})$(PSD-MK) are compared in a histogram plot. The notation $\tilde{R}(IVM1)$ (ZBM) indicates that this quantity was obtained from the experimental $R(IVM1)$ minus the theoretical $\vec{1}\,\vec{\tau}$ contribution calculated in the ZBM space. In many cases $\tilde{R}(IVM1)$ (ZBM) and $\tilde{R}(IVM1)$ (PSD-MK) are nearly equal and the conclusions do not strongly depend on which one is used.

For the strong transitions $\tilde{R}(IVM1)$ is on the average somewhat larger than R(GT). If we average the ratios $\tilde{R}(IVM1)/R(\mathrm{GT})$ for the transitions given in Table VII, we obtain 1.25, with an internal uncertainty of ± 0.10. Here we have summed the transition strengths for each nucleus given in Table VII and then computed the ratio. This result is insensitive to the choice of PSD-MK or ZBM results for $\tilde{R}(IVM1)$. Thus we have very clear evidence for a difference in the enhancement of $\vec{s}\,\vec{\tau}(M1)$ relative to $\vec{s}\,\vec{\tau}$(GT). This $25\pm 10\%$ difference between $\tilde{R}(IVM1)$ and R(GT) may arise from the mesonic exchange and pionic pair-current corrections which are much more important for the $M1$ operator than for the GT operator, as mentioned above.

From Table VII and Fig. 9 it can also be seen that the experimental R(GT) is on the average quenched (by about 20%) relative to the theoretical $R(\vec{s}\,\vec{\tau})$. This is presumably due to the many-$\hbar\omega$ configuration mixing and the delta-particle-nucleon-hole admixtures mentioned above.

In conclusion, near ^{16}O, the average "effective" $M1$ operator is close to the free nucleon value, but this is due to an accidental cancellation between a quenching effect (as seen for the GT operator) and an enhancement effect (due to exchange currents). About 20% of the $M1$ and GT contributions are due to "nuclear medium" effects which must be incorporated into the theory as effective two-body operators. These two-body "nuclear medium" effects provide a mechanism by which the 2p-2h 1^+

TABLE VII. Comparison of $M1$ and GT matrix elements.

		Experiment[a]					Theory—ZBM (Z int)				Theory—PSD (MK int)			
Mass	$J_i^\pi,T_i \rightarrow J_f^\pi,T_f$	E_f (MeV)	M(GT) or $M(pn)$	$M(IVM1)$ or $\mu(IV)$	$R(IVM1)$	R(GT) or $R(pn)$	$\tilde{R}(IVM1)$[b]	$R(s\tau)$	$R(l\tau)$	E_f (MeV)	$\tilde{R}(IVM1)$[b]	$R(s\tau)$	$R(l\tau)$	E_f (MeV)
13	$1/2^-,1/2 \rightarrow 1/2^-,1/2$	0.0	0.796(7)	−0.512	−0.66	0.78	−1.08	−1.00	4.00	0.0	−0.92	−0.92	2.50	0.0
14	$0^+,1 \rightarrow 1_1^+,0$	0.0	0.018	0.228(8)	0.17	0.017	0.50	0.89	−3.16	0.0	0.46	0.16	−2.71	0.0
	$\rightarrow 1_2^+,0$	3.95	2.22(13)	2.09(10)	1.58(8)	2.18(13)					1.85(8)	2.70	−2.54	3.90
	$\rightarrow 1_3^+,0$	6.20						1.01	1.84	4.11				
15	$1/2^-,1/2 \rightarrow 1/2^-,1/2$	0.0	0.897(7)	0.501	0.64	0.88	0.95	0.98	−2.88	0.0	1.06	1.00	−4.00	0.0
16	$0^+,0 \rightarrow 1_1^+,1$	16.22	0.08[c]	0.47(3)[d]	0.36(3)	0.08	0.13(3)	0.38	2.15	13.08	0.45(3)	0.026	−0.84	25.31
	$\rightarrow 1_2^+,1$	17.14	0.28[c]	0.60(4)[d]	0.46(3)	0.28	0.50(3)	0.44	−0.36	14.64	0.40(3)	0.028	0.59	26.33
	$\rightarrow 1_3^+,1$	18.8	0.26[c]	0.36(4)[e]	0.27(3)	0.26	0.21(3)	0.06	0.63	15.56	0.19(3)	0.078	0.81	28.19
16	$2^-,1 \rightarrow 1^-,0$	7.12	0.49(2)	1.52(9)[f]	1.14(7)	0.48(2)	1.12(7)	0.047	0.23	6.91	1.15(7)	0.088	−0.087	16.28
	$\rightarrow 2^-,0$	8.87	1.14(10)	3.69(14)[f]	2.78(11)	1.12(10)	2.10(11)	2.46	6.33	8.35	2.07(11)	1.66	6.68	19.30
	$\rightarrow 3^-,0$	6.13	1.02(1)	2.75(8)[f]	1.50(6)	1.00(1)	1.58(6)	1.54	−0.67	5.84	1.60(6)	0.92	−0.92	15.05
17	$5/2^+,1/2 \rightarrow 5/2^+,1/2$	0.0	3.168(7)	3.308	4.99	3.10	3.62	3.24	12.88	0.0	3.48	3.55	14.20	0.0
18	$0^+,1 \rightarrow 1_1^+,0$	0.0	2.209(4)	3.62(27)[g]	2.7(2)	2.16	2.3(2)	1.82	4.08	0.0	2.4(2)	2.86	2.94	0.0
	$\rightarrow 1_2^+,0$	1.70	0.51(4)	0.409(9)	0.303(9)	0.50(4)	0.485(9)	0.60	−1.74	1.71				
	$\rightarrow 1_3^+,0$	3.72	0.53[h]			0.52		0.19	1.27	3.50		0.09	3.06	3.06
18	$0^+,1 \rightarrow 1^+,2$	18.86		0.53(4)[i]	0.73(6)		0.62(6)	0.55	1.00	17.48				

[a]References 56 and 57 unless otherwise noted.
[b]$\tilde{R}(IVM1) = R(IVM1)_{exp} \pm 0.1062 R(l\tau)_{th}$.
[c]References 53 and 55.
[d]This work.
[e]Reference 12.
[f]We sum the decays of the 12.53 and 12.97 MeV 2^- states to obtain the isovector strength.
[g]Reference 58.
[h]Reference 54.
[i]Reference 60.

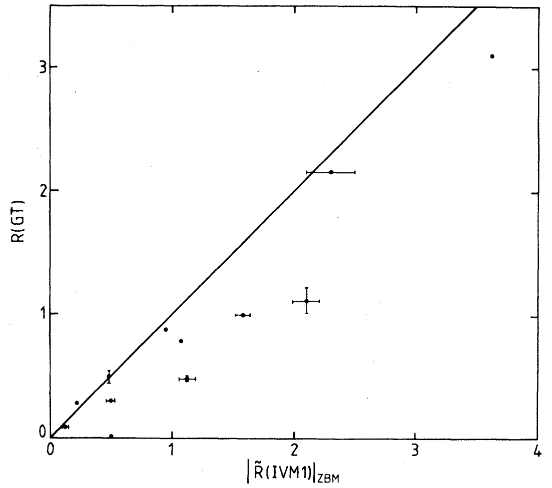

FIG. 8. A plot of the quantity $\tilde{R}(IVM1)$ on the x axis vs R(GT) on the y axis. $\tilde{R}(IVM1)$ was obtained from the experimental $R(IVM1)$ corrected for the $\vec{l}\,\vec{\tau}$ contribution calculated in the ZBM model (see Table VII and Sec. VI D). In the impulse approximation both quantities are equal to $R(\vec{s}\,\vec{\tau})$ and would lie on the 45° line shown.

states in ^{16}O can be directly excited from a closed-shell ground-state configuration. It may be necessary to include this effect in order to account for the experimental results, although a preliminary calculation[63] of exchange current contributions to the ^{16}O $M1$ transitions indicates they are too small to account for the observed effects.

E. 1p-1h states in $A=16$

It is instructive to consider the $M1$ and GT properties of known 0^- through 4^- low lying "1p-1h" states in $A=16$ since much data is available and the theories give some contrasting results. In addition to the GT results shown in Table VII, several other results are given in Table VIII.

In addition to the ZBM and PSD model spaces we have considered the simpler 1p-1h weak-coupling approximation in which, for example, the lowest 2^- state has a pure $(0p_{1/2})^{-1}(0d_{5/2})^1$ configuration. The $T=1$ to $T=0$ $B(M1)$ strengths in the weak-coupling model are very large (several W.u.), and larger than experiment. The ZBM and PSD model spaces can then be considered as two very different ways to expand the weak-coupling model space.

The ZBM model space contains the weak-coupling configurations for the 0^-, 1^-, 2^-, and 3^- states and adds the 3p-3h configurations. Even though the ZBM wave functions admix up to about 30% of the 3p-3h component into the lowest levels, the $B(M1)$ values are nearly the same as in the pure weak coupling. The main reason for this is that the

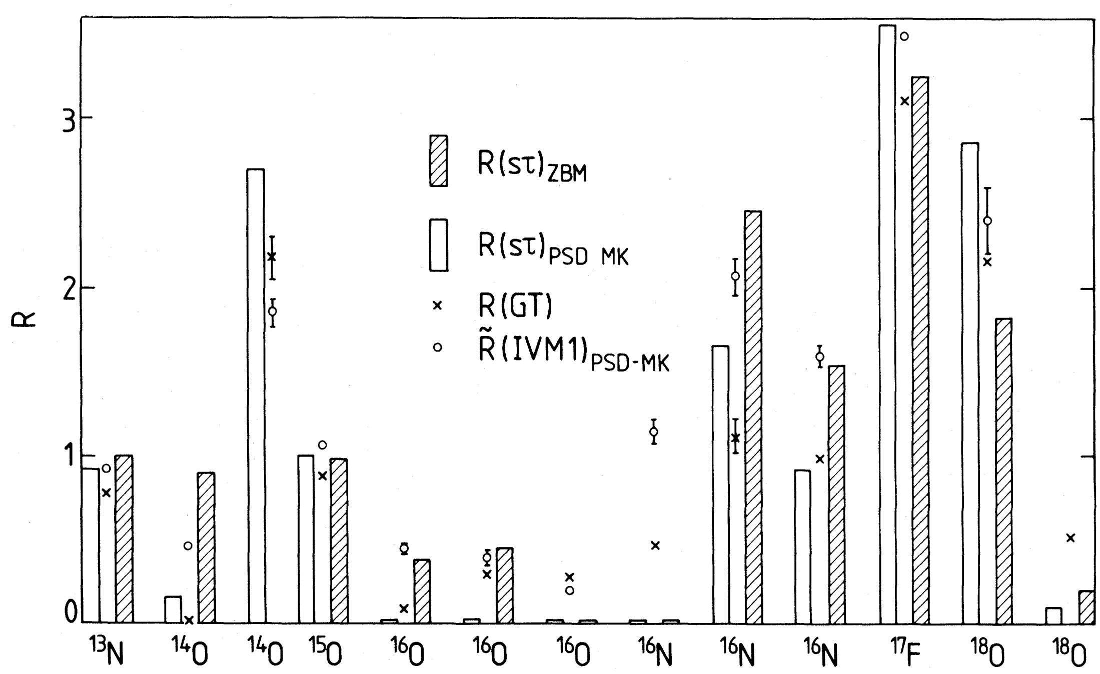

FIG. 9. Comparisons of the experimental matrix elements R(GT) (crosses) and $\tilde{R}(IVM1)$ (open circles), and the theoretical matrix elements $R(\vec{s}\,\vec{\tau})$ (unshaded histograms for ZBM and shaded histograms for PSD-MK). $\tilde{R}(IVM1)$ was obtained from the experimental $R(IVM1)$ corrected for the $\vec{l}\,\vec{\tau}$ contribution calculated in the PSD-MK model (see Table VII and Sec. VI D).

TABLE VIII. $M1$ transition strengths between the lowest negative parity states of each spin in $A=16$. $B(M1)$ in units of $\mu_N{}^2$ and $\mu(J)$ in units of μ_N.

	Experiment[a]			Theory $B(M1)$ or μ		
$J_i(T_i)\to J_f(T_f)$	E_i (MeV)	E_f (MeV)	$B(M1)$ or μ	jj coupling	ZBM Z int	PSD MK int
^{16}O $4^-(1)\to 4^-(0)$				11.49		11.49
$\to 3^-(0)$	19.0	6.13	0.29(13)[b]	1.41		0.41
$3^-(1)\to 4^-(0)$				1.81		1.60
$\to 3^-(0)$	13.26	6.13	2.20(36)	2.68	2.28	1.31
$\to 2^-(0)$				0.50	0.52	0.20
$2^-(1)\to 3^-(0)$	12.53[c] 12.97	6.13	1.51(9)	0.70	0.76	0.24
$\to 2^-(0)$		8.87	2.72(22)	4.21	3.47	1.97
$\to 1^-(0)$		7.12	0.46(6)	0	0.0018	0.0021
$1^-(1)\to 2^-(0)$				0	0.0049	0.044
$\to 1^-(0)$	13.09	7.12	0.56(16)	1.73	1.46	0.64
$\to 0^-(0)$				1.88	1.75	2.05
$0^-(1)\to 1^-(0)$	12.80	7.12	1.18(9)	5.63	5.09	1.44
$2^-(0)\to 3^-(0)$	8.87	6.13	0.0036(14)	0.0057	0.0053	0.00025
$0^-(0)\to 1^-(0)$	10.95	7.12	0.0012(8)	0.046	0.040	0.0117
^{16}N $3^-(1)\to 2^-(1)$	0.30	0.0	0.016(1)[d]	0.0056	0.00055	0.033
$1^-(1)\to 2^-(1)$	0.40	0.0	0.037(3)[e]	0	0.0022	0.017
$1^-(1)\to 0^-(1)$	0.40	0.12	0.299(24)[e]	0.65	0.40	0.50
$\mu[3^-(1)]$	0.30		$\pm 1.52(9)$[d]	-2.18	-2.01	-1.43
$\mu[2^-(1)]$	0.0			-1.55	-1.46	-2.13
$\mu[1^-(1)]$	0.40		$\pm 1.83(13)$[e]	-2.18	-1.80	-1.98

[a]References 56 and 57 unless otherwise noted.
[b]This work.
[c]We sum the decays of the 12.53 and 12.97 MeV 2^- states to obtain the isovector strength.
[d]Reference 62.
[e]Reference 61.

$M1$ operator does not connect the off-diagonal 1p-1h and 3p-3h components. Millener has made calculations which include 3p-3h admixtures in the larger PSD space and found a similar result.[20]

On the other hand, in PSD all but the 4^- 1p-1h states are mixed by the MK interaction. This mixing has the effect of reducing the $B(M1)$ values and improving the agreement with experiment, rather dramatically in some cases. (This reduction can be associated with the tendency towards LS coupling.) There remain, however, some glaring discrepancies. The experimental transition strengths for all three branches of the $M1$ and GT decay of the 2^- $T=1$ state are larger than the PSD-MK theory. In particular, the decay of this state to the 1^- $T=0$ state is experimentally not nearly as forbidden as expected. This transition is completely forbidden in the j-j weak coupling limit because it involves only the $0d_{5/2}$ to $1s_{1/2}$ single-particle matrix element.

F. The 1^+ $T=1$ states in $A=16$

Some transitions to and from the 1^+ $T=1$ states in $A=16$ are shown in Fig. 10. As expected, the beta decays of ^{16}C to ^{16}N(1^+) are stronger than the $M1$ decays ^{16}O(1^+) to ^{16}O(g.s.) because the beta decay connects two states each of which is predominantly 2p-2h, while the gamma decay connects a "2p-2h" state with a state which is predominantly 0p-0h. In addition, there are data on the ^{16}O(p,n) reactions feeding the 1^+ states.[53,55]

In the ZBM space the lowest 1^+ $T=1$ state is calculated to occur at 13.08 MeV and 15.52 MeV with the "Z" and "F" interactions, respectively. The agreement with the experimental energy of 16.22 MeV is reasonable but not too surprising since these interactions have been adjusted to fit (among many binding energy observables) the spectrum of many-particle-many-hole states in ^{16}O. In the PSD model

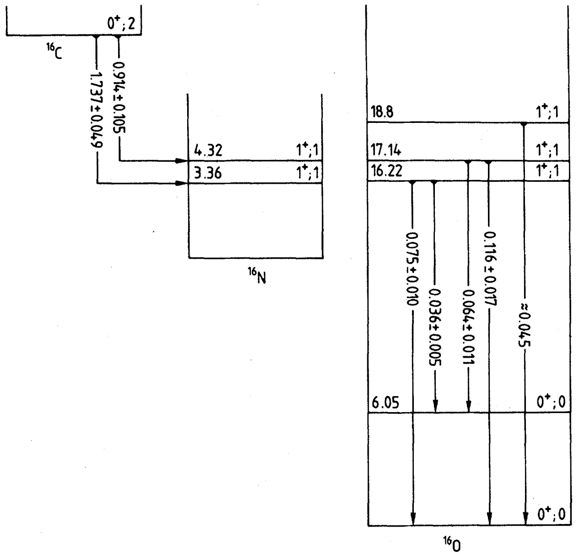

FIG. 10. Experimental $M1$ and GT decay strengths involving the $A=16$ 1^+ $T=1$ states. The reduced transition strengths B(GT) are dimensionless and $B(M1)$ are in units of $\mu_N{}^2$.

space the excitation energies depend on the type of configurations allowed. With the MK interaction the excitation energy relative to the closed-shell configuration for the g.s. is 17.10 MeV, in good agreement with experiment. When 2p-2h admixtures are also allowed in the g.s. its binding energy increases by 8.21 MeV, thus putting the 1^+ at 25.31 MeV excitation, much higher than experiment. The spacings between the lowest five 1^+ $T=1$ levels are about the same in the ZBM and PSD calculations, and the agreement of the spacings with the three states known experimentally is good (see Table IX).

The predicted and measured $M1$, GT, and (p,n) strengths involving the 1^+ states are given in Table IX. The lowest two 1^+ states are also both relatively strongly populated in the ^{14}N(t,p) (Refs. 64 and 65) and ^{14}C(^{3}He,p) (Refs. 64 and 66) reactions. The measured relative two-particle stripping strengths along with the predictions are given in Table X. The ZBM calculation is in reasonable agreement with all of these strengths. On the other hand, the PSD-MK theory gives poorer agreement for each observable. In particular, it greatly underpredicts the GT and $M1$ strength. We have repeated the PSD calculation with the Arima-Strottman interac-

TABLE IX. Comparison of observed $E1$, $M1$, GT, and (p,n) transition rates with shell model calculations: Transitions involving the 1^+ $T=1$ states in $A=16$.

	Experiment			Theory ZBM (Z int)			Theory PSD (MK int)		
Transition	E_i (MeV)[a]	E_f (MeV)	B[b]	E_i (MeV)[a]	E_f (MeV)	B[b]	E_i (MeV)[a,c]	E_f (MeV)	B[b]
^{16}C$(0_1^+)\rightarrow{}^{16}N(1_1^+)$	[22.71]	3.36	1.737 ± 0.048[d]	[18.53]	2.25	2.103	[23.18]	3.55	0.002
$\rightarrow{}^{16}$N(1_2^+)		4.32	0.914 ± 0.105[d]		3.81	3.418		4.57	0.567
^{16}O$(1_1^+)\rightarrow{}^{16}O(0_1^+)$	16.22	0	0.075 ± 0.010[e]	13.08	0	0.218	17.10	0	0.0024
$\rightarrow{}^{16}$O(0_2^+)		6.05	0.036 ± 0.005[e]		6.19	0.098			
$\rightarrow{}^{16}$O(2_1^+)		6.92	$0.040^{+0.022}_{-0.038}$[e]		7.39	0.148			
$\rightarrow{}^{16}$O(1_1^-)		7.12	$0.0005^{+0.0003}_{-0.0005}$[e]		6.91	0.020			
^{16}O$(1_2^+)\rightarrow{}^{16}O(0_1^+)$	17.14	0	0.116 ± 0.017[e]	14.64	0	0.095	18.12	0	0.0048
$\rightarrow{}^{16}$O(0_2^+)		6.05	0.064 ± 0.011[e]		6.19	0.109			
$\rightarrow{}^{16}$O(2_1^+)		6.92	≤0.033[e]		7.39	0.001			
$\rightarrow{}^{16}$O(1_1^-)		7.12	≤0.0004[e]		6.91	0.001			
^{16}O$(1_3^+)\rightarrow{}^{16}O(0_1^+)$	18.8	0	≈0.047[f] 0.043 ± 0.010[g]	15.57	0	0.010	19.98	0	0.016
^{16}O$(1_4^+)\rightarrow{}^{16}O(0_1^+)$				16.49	0	0.044	20.42		0.0001
^{16}O$(0_1^+)\rightarrow{}^{16}F(1_1^+)$	0	3.76	0.006[h]	0	2.25	0.14	0	3.55	0.0007
$\rightarrow{}^{16}$F(1_2^+)	0	4.65	0.078[h]	0	3.81	0.19	0	4.57	0.0008
$\rightarrow{}^{16}$F(1_3^+)	0	6.2	0.068[h]	0	4.74	0.0036	0	6.43	0.006

[a]Excitation energy in ^{16}O.
[b]B(GT) is dimensionless and includes the factor $(g_A/g_V)^2$ as defined in text; $B(M1)$ in units of $\mu_N{}^2$, $B(E1)$ in units of e^2fm^2.
[c]8.21 MeV has been subtracted from the theoretical energies (see Sec. VI E).
[d]References 56 and 57.
[e]This work.
[f]Reference 1.
[g]Reference 12.
[h]References 53 and 55.

TABLE X. Summary of (t,p) and $(^3He,p)$ reactions to the ^{16}N 1^+ $T=1$ states.

No.	$\sigma[^{14}N(t,p)]$ Exp[a] (%)	ZBM[c] (Z int) (%)	PSD (MK int) (%)	$\sigma[^{14}C(^3He,p)]$ Exp[b] (%)	ZBM[c] (Z int) (%)	PSD[c] (MK int) (%)	Excitation energy (MeV) Exp	ZBM (Z int)	PSD (MK int)
1	27	20	64	30	52	5	3.36	2.25	3.55
2	23	27	6	20	15	47	4.32	3.81	4.57
3		0	3		3	5	5.9	4.74	6.43
4		47	3		0	1		5.66	6.87
$\Sigma 1-4$		94	76		70	58			

[a]Experimental values from Refs. 64 and 65 arbitrarily normalized to 50% for the sum of the 3.36 and 4.32 MeV 1^+ states in ^{14}N.

[b]Experimental values from Refs. 64 and 66 arbitrarily normalized to 50% for the sum of the 3.36 and 4.32 MeV 1^+ states in ^{14}N.

[c]Theoretical values normalized to 100% for the sum over all states.

tion and find results very similar to those with the MK interaction. We cannot reproduce the results shown in Fig. 2 of Ref. 40.

To gain more insight into the reason for the failure of the PSD calculations we have calculated the $M1$ and GT strengths to a wide range of excitation energies in ^{16}O. It turns out in the PSD space calculations that the $M1$ strength is spread rather uniformly over about 100 states, and it is neither convenient nor informative to present such results in tabular form. Thus, we present the results by making a Gaussian average over the levels and showing a plot of the $M1$ strength distribution ($M1$SD) versus excitation energy. A full width at half maximum of 0.9 MeV for the Gaussian was chosen because a narrower width tended to show more fine structure than we believe is physically meaningful.

The $M1$SD for the ^{16}O g.s. 0^+ to 1^+ $T=1$ states is shown in Fig. 11. The corresponding summed $M1$SD are given in Table XI. In order to directly show the division of the $M1$SD into spin and orbital contributions, the calculations were repeated with the orbital g factors set to zero, and the results are plotted in Fig. 12. For this latter case we compare to the experimental (p,n) data of Refs. 53 and 55 by multiplying the $B(pn)$ values by 1.690 (which accounts for the g factors and isospin Clebsch-Gordan coefficients). By comparing Figs. 11 and 12 it can be seen that without the orbital contribution the $M1$SD is reduced by about half in the ZBM model.

The PSD calculation is in much poorer agreement with experiment than is the ZBM calculation for both the $M1$'s in ^{16}O and the GT decays of ^{16}C (see Fig. 13). Could this discrepancy be due to the neglect of 4p-4h configurations in the PSD calculations? To explore this we repeated the ZBM calculations without the 4p-4h configurations in the 0^+ and 1^+ states. The comparisons (Figs. 11–13) show that although the details of the $M1$SD structure are sensitive to these 4p-4h configurations, the summed strengths are similar. This is reasonable since there is less than 6% intensity of the 4p-4h component in the ZBM ground state. Hence the problem must be with the 2p-2h configurations.

The most important reason for the difference between the $M1$SD's predicted with the PSD and ZBM interactions is the difference in the ground state wave functions. We demonstrate this by comparing a calculation of $M1$ strength from the ZBM (0p-0h + 2p-2h) and MK PSD ground states to the MK PSD 1^+ $T=1$ levels. The ZBM ground state gives a considerably larger $M1$ strength than the MK ground state (see Figs. 11 and 12). The main difference between the MK and ZBM ground states is not the total intensity of 2p-2h components (which are 25% for ZBM and 21% for PSD), but rather lies in the structure of the 2p-2h component. In going from ZBM to PSD the $(0p_{1/2})^{-2}(0d_{5/2})^2$ component gets reduced from 24% to 3.5%, with the next largest component being

$$(0p_{3/2})^{-1}(0p_{1/2})^{-1}(0d_{5/2})^1(0d_{3/2})^1 .$$

We conclude that the calculated $M1$SD is quite sensitive to some as yet uncontrolled aspect of the interactions.

Although the lowest two 1^+ states have quite similar $B(M1)$, B(GT), and two-particle transfer strengths, it is interesting that the low-lying 1^+ states are predicted to have very different inelastic electron scattering form factors (see Fig. 14). It would be very interesting to see if this is substantiated by experiment.

Because of the success of the ZBM model in accounting for the ^{16}O 1^+ states, we have also calculated the GT observables for several $A=15$–18 nu-

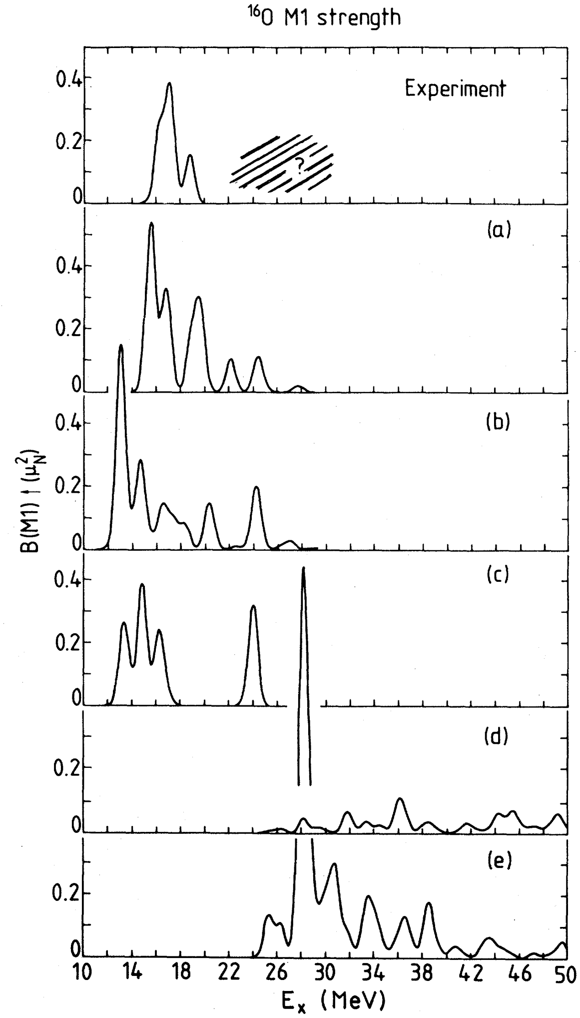

FIG. 11. Distribution of $B(M1$, 0^+ g.s. to 1^+ $T=1)$ strength in ^{16}O vs excitation energy in MeV. The experiment is shown at the top followed by the various theoretical calculations. For both experiment and theory, the $B(M1)$ values for discrete states have been averaged over a Gaussian (with FWHM=0.94 MeV) in order to emphasize the general trends. The vertical scale has been adjusted so that the $B(M1)$ value for an isolated peak can be simply read off from the maximum. (a) The ZBM model-space results with the "F" interaction. (b) The ZBM model-space results with the "Z" interaction. (c) Same as (b) except excluding 4p-4h configurations. (d) The PSD model-space results with the "MK" interaction. (e) The 0^+ g.s. as in (c) and the 1^+ $T=1$ state as in (d).

clei. As can be seen from Table XII, the ZBM model continues to give rough qualitative agreement with experiment. One may compare a few of the measured transitions in Table V with shell model

TABLE XI. Total sums of the strength distributions shown in Figs. 11–13 and % 2p-2h admixture in the ^{16}O ground state. $B(M1)$ in units of $\mu_N{}^2$.

Calculation	(a)	(b)	(c)	(d)	(e)
$\Sigma B(M1,0^+T=0\rightarrow 1^+T=1)$ $(g_l^{(1)}=0.5)$	1.65	1.56	1.24	1.00	3.44
$\Sigma B(M1,0^+T=0\rightarrow 1^+T=1)$ $(g_l^{(1)}=0.0)$	0.79	0.70	0.70	0.70	3.32
$\Sigma B(\mathrm{GT},0^+T=2\rightarrow 1^+T=1)$	8.40	8.66	8.15	17.8	16.1
% 2p-2h in 0^+ $T=0$	34	30	25	21	25

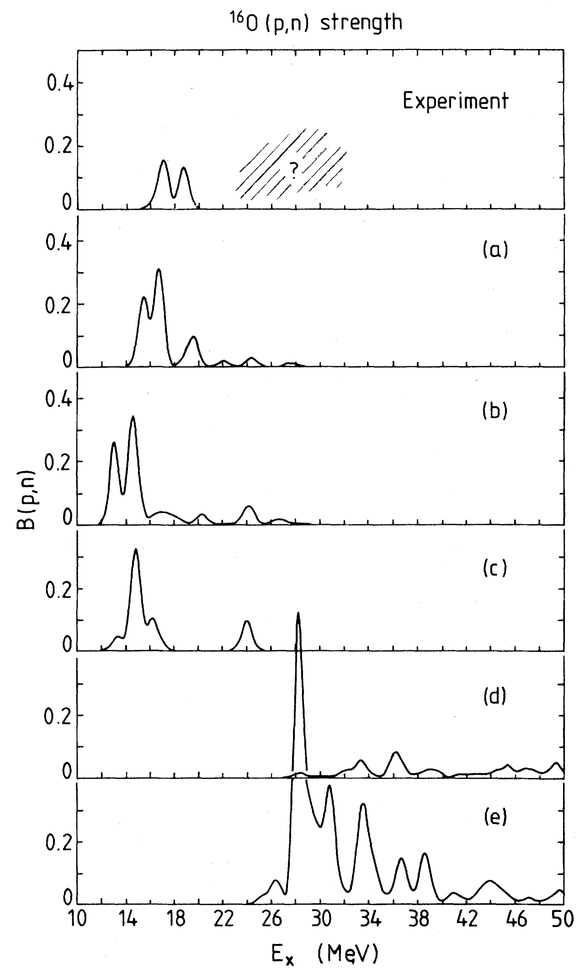

FIG. 12. Distribution of $NB(pn$, 0^+ g.s. to 1^+ $T=1)$ strength in ^{16}O (see caption to Fig. 1). The theory is the same as in Fig. 1 except that the orbital g factors have been set equal to zero. The experimental (p,n) cross sections from Refs. 53 and 55 were normalized to the strong ^{12}N to ^{12}C B(GT) value and then multiplied by the factor $N=1.690$ so that they can be compared in an absolute manner to the theoretical $B(M1)$ with $g_l=0$.

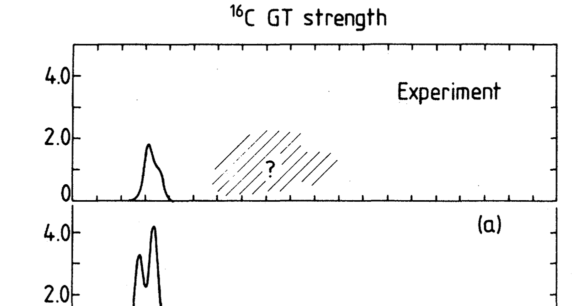

FIG. 13. Distribution of ^{16}C(g.s.) to ^{16}N($1^+,T=1$) B(GT) strength. The excitation energies of the 1^+ states are given relative to the ^{16}O g.s. as in Fig. 11. The theoretical calculations are as given in the caption to Fig. 11.

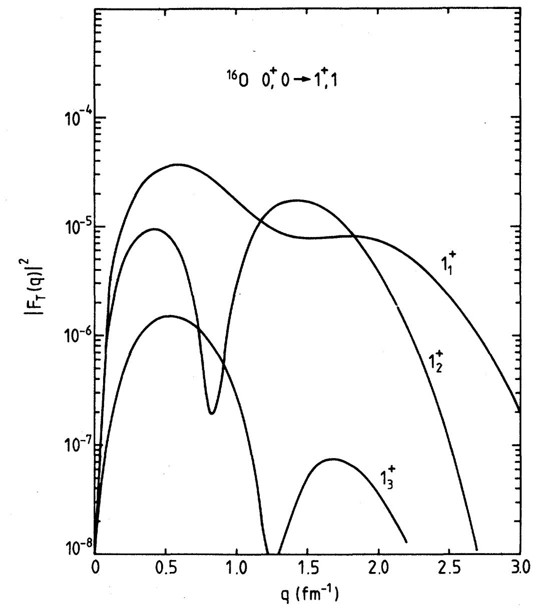

FIG. 14. Transverse $M1$ electron scattering form factors for the lowest three 1^+ states in ^{16}O obtained in the ZBM model with the Z interaction.

calculations. This is done in Table XIII, where again one finds only very rough agreement.

VII. CONCLUSIONS

In our comparisons between experiment and theory we have first focused on the relationships between the Gamow-Teller and isovector $M1$ matrix elements. The experimental GT matrix elements for the strong transitions are on the average quenched about 20% relative to shell-model calculations, which allow for full mixing within the major oscillator shells. At present it is not clear theoretically whether this is mostly due to delta-particle-nucleon-hole or to many-$\hbar\omega$ nuclear configuration mixing.[49] For the $M1$ matrix elements we have used theory to make a separation between $\vec{s}\,\vec{\tau}$ and $\vec{l}\,\vec{\tau}$ contributions. In those cases for which the $\vec{l}\,\vec{\tau}$ contribution is not very important, the experimental $M1$ matrix elements are on the average not quenched. We have shown clear evidence for the enhancement of $\vec{s}\,\vec{\tau}(M1)$ relative to $\vec{s}\,\vec{\tau}$(GT). Since the mechanisms which give rise to the quenching in GT decays affect the $\vec{s}\,\vec{\tau}$ part of the $M1$ operator in exactly the same way, the observed average $25\pm10\%$ enhancement of $\vec{s}\,\vec{\tau}(M1)$ relative to $\vec{s}\,\vec{\tau}$(GT) is presumably due to the meson-exchange and pair-current contributions.[50]

We then investigated several truncation schemes for shell model calculations of $1\hbar\omega$ excitations around $A=16$. Here, as expected, calculations in the complete PSD space ($0p_{1/2}$, $0p_{3/2}$, $0d_{5/2}$, $1s_{1/2}$, and $0d_{3/2}$) are much more successful in reproducing $M1$ and GT observables involving the predominantly 1p-1h states than is the ZBM calculation (which allows many-particle many-hole excitations in a space restricted to $0p_{1/2}$, $0d_{5/2}$, and $1s_{1/2}$). Yet even for these simple "1p-1h" states the PSD calculations with the MK interaction have striking failures—the most conspicuous example being the ^{16}N→ ^{16}O($1^-;T=0$) beta decay. This reveals deficiencies in the $1\hbar\omega$ part of the MK residual interaction.

Then we turned to the next simplest test case—the

TABLE XII. Comparison of GT transition rates with the ZBM shell model calculations: Transitions in $A=15$, 17, and 18.

Transition	Experiment[a] E_f (MeV)	B(GT)[b]	Theory (Z int) E_f (MeV)	B(GT)[b]
$^{15}C\rightarrow^{15}N(1/2_1^+)$	5.30	0.514±0.012	4.60	0.770
$(3/2_1^+)$	7.30	$(7.96\pm0.92)\times10^{-4}$	6.48	0.554
$(1/2_2^+)$	8.31	0.041±0.005	6.98	0.013
$(3/2_2^+)$	8.57	0.028±0.005	7.28	2.1×10^{-5}
$(1/2_3^+)$	9.05	0.551±0.051	9.56	1.95
$^{17}N\rightarrow^{17}O(1/2_1^-)$	3.06	$(5.14\pm0.95)\times10^{-4}$	2.33	0.015
$(3/2_1^-)$	4.55	0.246±0.011	4.11	1.182
$(3/2_2^-)$	5.38	0.814±0.038	4.79	1.449
$(1/2_2^-)$	5.94	0.303±0.028	5.04	0.770
$^{18}N\rightarrow^{18}O(1_1^-)$	4.46	0.044±0.006	4.10	0.068
(2_1^-)	5.53	0.004±0.001	5.20	0.015
(1_2^-)	6.20	0.003±0.001	6.44	0.059
(2_2^-)	6.35	0.005±0.001	5.97	0.068
(0_1^-)	6.88	0.040±0.007	5.85	0.264
(2_3^-)	7.77	0.030±0.006	7.36	0.042

[a]References 56, 57, and 59.
[b]Includes the factor $(g_A/g_V)^2$ as defined in the text.

largely 2p-2h 1^+ $T=1$ and 0^+ $T=2$ states. Here neither the ZBM nor the PSD calculations can quantitatively describe the $M1$ and GT transitions involving the 1^+ states. However, the ZBM model gives much better qualitative agreement than does the PSD model. Both the GT decays of ^{16}C and $M1$ decays of ^{16}O(1^+) to the ground and "4p-4h" 0^+ states are explained to within a factor of 3 or better by the ZBM calculation. In contrast, the PSD model predicts much too small $M1$ and GT strengths. In the case of the $M1$ transitions, we have shown that this can be caused by a deficiency in the ^{16}O ground state wave function as computed with the MK interaction. Although both the ZBM and PSD models have comparable intensities for the total 2p-2h component in the ^{16}O ground state, the form of these components is very different in the ZBM and PSD-MK calculations. Although this failure of the MK interaction may in part reflect the above-mentioned problems with the $1\hbar\omega$ residual matrix elements, it very probably reveals a serious shortcoming in the $2\hbar\omega$ matrix elements as well.

Clearly more work remains to be done. Which features of the MK interaction produce the wrong form of the 2p-2h components in the ^{16}O ground state? The calculations predict that most of the $M1$ strength built on the ^{16}O ground state lies above $E_x=19$ MeV—an area that is currently unexplored. Is this in fact correct? Finally, it would be valuable to have more data which can help characterize the n-particle-n-hole character of the states in ^{16}O. Is the "2p-2h" 0^+ $T=0$ state the one at 12.0 MeV or does it lie higher?

Understanding the structure of ^{16}O is a central item on the agenda of nuclear structure physics. A number of challenging problems must be solved be-

TABLE XIII. A comparison of some $\Delta T=1$ $E1$ and $M1$ transitions in ^{16}O with ZBM calculations.

Transition	Experiment E_i (MeV)	E_f (MeV)	$B(E1$ or $M1)$[a]	Theory (Z int) E_i (MeV)	E_f (MeV)	$B(E1$ or $M1)$[a]
$2_1^+,1\rightarrow3_1^-,0$	16.45	6.13	0.010 e^2fm^2	13.85	5.84	0.003 e^2fm^2
$3_1^+,1\rightarrow3_1^-,0$	16.82	6.13	7×10^{-4} e^2fm^2	14.19	5.84	0.008 e^2fm^2
$\rightarrow2_1^+,0$		6.92	0.11 μ_N^2		7.39	0.21 μ_N^2
$2_2^-,1\rightarrow1_1^-,0$	17.88	7.12	0.14 μ_N^2	15.26	6.91	0.015 μ_N^2

[a]$B(E1)$ computed assuming $e_p^{\rm eff}-e_n^{\rm eff}=0.5e$. Note: 1 W.u. $(M1)=1.79$ μ_N^2 and, for $A=16$, 1 W.u. $(E1)=0.41$ e^2fm^2.

fore we have a predictive theory of nuclei. Fortunately the problem is becoming well focused and we may look forward to some progress in this important area.

ACKNOWLEDGMENTS

We thank Dr. D. J. Millener, who has been most generous in providing many comments and calculations, and Dr. E. F. Garman for help with proofreading. K.A.S. acknowledges support by the United Kingdom S.E.R.C. as a Senior Visiting Fellow during part of this work. E.G.A. is grateful for a J.S. Guggenheim Fellowship which made possible a very productive visit to Oxford University. This work was supported in part by the U.S. Department of Energy.

[1]S. Cohen and D. Kurath, Nucl. Phys. 73, 1 (1965).

[2]B. M. Preedom and B. H. Wildenthal, Phys. Rev. C 6, 1633 (1972).

[3]K. A Snover, P. G. Ikossi, and T. A. Trainor, Phys. Rev. Lett. 43, 117 (1979); and private communication.

[4]S. H. Chew, J. Lowe, J. M. Nelson, and A. R. Barnett, Nucl. Phys. A229, 241 (1974).

[5]S. H. Chew, J. Lowe, J. M. Nelson, and A. R. Barnett, Nucl. Phys. A286, 451 (1977).

[6]A. R. Barnett and N. W. Tanner, Nucl. Phys. A152, 257 (1970).

[7]R. E. Marrs, Ph.D. dissertation, University of Washington, 1975; R. E. Marrs, E. G. Adelberger, and K. A. Snover, Phys. Rev. C 16, 61 (1977).

[8]F. C. Barker, G. D. Symons, N. W. Tanner, and P. B. Treacy, Nucl. Phys. 45, 449 (1963).

[9]P. M. Endt, Nucl. Data Tables 23, 3 (1979).

[10]H. Miska *et al.*, Phys. Lett. 58B, 155 (1975).

[11]F. Ajzenberg-Selove, Nucl. Phys. A375, 1 (1982).

[12]G. Küchler, H.-D. Gras, A. Richter, E. Spamer, W. Steffen, and W. Knüpfer, Nucl. Phys. (to be published).

[13]C. Rolfs and W. S. Rodney, Nucl. Phys. A235, 450 (1974).

[14]K. A. Snover, P. G. Ikossi, and K. T. Lesko, University of Washington Annual Report, 1980 (unpublished), p. 80.

[15]H. Breuer, G. J. Wagner, K. T. Knöpfle, G. Mairle, and P. Doll, Phys. Lett. 96B, 35 (1980).

[16]G. Mairle, G. J. Wagner, P. Doll, K. T. Knöpfle, and H. Breuer, Nucl. Phys. A299, 39 (1978).

[17]R. S. Henderson, B. M. Spicer, I. D. Svalbe, V. C. Officer, G. G. Shute, D. W. Devins, D. L. Friesel, W. P. Jones, and A. C. Attard, Aust. J. Phys. 32, 411 (1979).

[18]D. B. Holtkamp, W. J. Braithwaite, W. Cottingame, S. J. Greene, R. J. Joseph, C. Fred Moore, C. L. Morris, J. Piffaretti, E. R. Siciliano, H. A. Thiessen, and D. Dehnhard, Phys. Rev. Lett. 45, 420 (1980).

[19]I. Sick, E. B. Hughes, T. W. Donnelly, J. D. Walecka, and G. E. Walker, Phys. Rev. Lett. 23, 1117 (1969); see also F. Petrovitch, in *Proceedings of the International Conference on Nuclear Physics, Berkeley, 1980,* edited by R. M. Diamond and J. O. Rasmussen (North-Holland, Amsterdam, 1981), p. 499.

[20]J. Millener, private communication.

[21]M. Stroetzel and A. Goldmann, Z. Phys. 233, 245 (1970).

[22]L. L. Ames, Phys. Rev. C 25, 729 (1982).

[23]K. A. Snover, E. G. Adelberger, and D. R. Brown, Phys. Rev. Lett. 32, 1061 (1974).

[24]S. Jausel-Hüsken and H. Freiesleben, Z. Phys. A 285, 363 (1977).

[25]A. R. Barnett, Nucl. Phys. A120, 342 (1968).

[26]A. M. Baxter, P. G. Ikossi, A. M. McDonald, and J. A. Kuehner, Nucl. Phys. A305, 213 (1978).

[27]N. M. Tanner, G. C. Thomas, and E. D. Earle, Nucl. Phys. 52, 29 (1964).

[28]G. Dearnaley, D. S. Gemmell, B. W. Hooton, and G. A. Jones, Phys. Lett. 1, 260 (1962).

[29]A. Goldmann and M. Stroetzel, Phys. Lett. 31B, 287 (1970).

[30]S. H. Chew, J. Lowe, J. M. Nelson, and A. R. Barnett, Nucl. Phys. A298, 19 (1978).

[31]G. D. Dracoulis and G. J. F. Legge, Nucl. Phys. 177, 241 (1971).

[32]D. Robson, Nucl. Phys. A308, 381 (1978).

[33]T. Engeland, Nucl. Phys. 72, 68 (1968); G. E. Brown and A. M. Green, Phys. Lett. 15, 168 (1965); Nucl. Phys. 75, 401 (1966).

[34]V. Gillet, Nucl. Phys. 51, 410 (1964).

[35]D. J. Millener and D. Kurath, Nucl. Phys. A255, 315 (1975).

[36]A. P. Zucker, B. Buck, and J. B. McGrory, Phys. Rev. Lett. 21, 39 (1968).

[37]A. P. Zucker, Phys. Rev. Lett. 23, 983 (1969).

[38]B. S. Reehal and B. H. Wildenthal, Part. Nucl. 6, 137 (1973).

[39]J. B. McGrory and B. H. Wildenthal, Phys. Rev. C 7, 974 (1973).

[40]A. Arima and D. Strottman, Phys. Lett. 96B, 23 (1980).

[41]T. T. S. Kuo and G. E. Brown, Nucl. Phys. A114, 241 (1968); G. E. Brown and T. T. S. Kuo, *ibid.* A92, 481 (1967).

[42]T. T. S. Kuo and G. E. Brown, Nucl. Phys. 85, 40 (1966).

[43]J. P. Elliott and T. H. R. Skyrme, Proc. R. Soc. London A232, 561 (1955).

[44]D. H. Gloeckner and R. D. Lawson, Phys. Lett. 53B, 313 (1974).

[45]J. B. McGrory and B. H. Wildenthal, Phys. Lett. 60B, 5 (1975).

[46]D. H. Wilkinson, Nucl. Phys. A209, 470 (1973).

[47]K. Shimizu, M. Ichimura, and A. Arima, Nucl. Phys. A226, 282 (1974); H. Hyuga, A. Arima, and K. Shimizu, *ibid.* A336, 363 (1980); A. Arima and H. Hyuga, in *Mesons and Nuclei,* edited by M. Rho and D. Wilkinson (North-Holland, Amsterdam, 1979), Vol. II, p. 683.

[48]M. Ericson, A. Figureau, and C. Thevenet, Phys. Lett. 45B, 19 (1973); M. Rho, Nucl. Phys. A231, 493 (1974); K. Ohta and M. Watamatsu, *ibid.* A234, 445 (1974); E. Oset and M. Rho, Phys. Rev. Lett. 42, 47 (1979); I. S. Towner and F. C. Khanna, Phys. Rev. Lett. 42, 51 (1979); A. Bohr and B. R. Mottelson, Phys. Lett. 100B, 10 (1981); A. Harting, W. Weise, H. Toki, and A. Richter, *ibid.* 104B, 261 (1981); T. Suzuki, S. Krewald, and J. Speth, *ibid.* 107B, 9 (1981).

[49]A. Arima, in Proceedings of the International Conference on Spin Excitations in Nuclei, Telluride, 1982 (unpublished).

[50]M. Chemtob and M. Rho, Nucl. Phys. A173, 1 (1971).

[51]R. R. Doering, A. Galonsky, D. M. Patterson, and C. F. Bertsch, Phys. Rev. Lett. 35, 1691 (1975); D. E. Bainum, J. Rapaport, C. D. Goodman, D. J. Horen, C. C. Foster, M. B. Greenfield, and C. A. Goulding, *ibid.* 44, 1751 (1980); B. D. Anderson, J. N. Knudson, P. C. Tandy, J. W. Watson, R. Madey, and C. C. Foster, *ibid.* 45, 699 (1980); D. J. Horen *et al.*, Phys. Lett. 95B, 27 (1980); W. A. Sterrenburg, S. M. Austin, R. P. DeVito, and A. Galonsky, *ibid.* 45, 1839 (1980); D. J. Horen *et al.*, *ibid.* 99B, 383 (1981).

[52]F. Petrovich, in *The (p,n) Reaction and the Nucleon-Nucleon Force,* edited by C. D. Goodman *et al.* (Plenum, New York, 1980), p. 115; C. D. Goodman, C. A. Goulding, M. B. Greenfield, J. Rapaport, D. E. Bainum, C. C. Foster, W. G. Love, and F. Petrovich, Phys. Rev. Lett. 44, 1745 (1980).

[53]A. Fazely, B. D. Anderson, M. Ahmed, A. R. Baldwin, A. M. Kalenda, W. Bertozzi, T. N. Buti, J. M. Finn, M. A. Kovash, B. Hugh, and C. C. Foster, Phys. Rev. C 25, 1760 (1982).

[54]B. D. Anderson, A. Fazely, R. J. McCarthy, P. C. Tandy, J. W. Watson, R. Madey, W. Bertozzi, T. N. Buti, J. M. Finn, J. Kelly, M. A. Kovash, B. Pugh, B. H. Wildenthal, and C. C. Foster, Phys. Rev. C (to be published).

[55]B. D. Anderson, R. J. McCarthy, M. Ahmad, A. Fazely, A. M. Kalenda, J. N. Knudson, J. W. Watson, R. Madey, and C. C. Foster, Phys. Rev. C 26, 8 (1982). We have obtained $B(pn)$ values from this work by normalizing the cross sections to the experimental ^{12}N(1^+) to ^{12}C(0^+, g.s.) GT decay strength of $B(\mathrm{GT})=0.412(2)$ so that $B(pn)=\sigma(p,n)/9.28N_d$.

[56]P. M. Endt, At. Data Nucl. Data Tables 23, 3 (1979).

[57]F. Ajzenberg-Selove, Nucl. Phys. A360, 1 (1981); A375, 1 (1982); A300, 1 (1982).

[58]J. Keinonen, H. N. Mak, T. K. Alexander, G. C. Ball, W. G. Davies, J. S. Foster, and I. V. Mitchell, Phys. Rev. C 23, 2073 (1981).

[59]J. W. Olness, E. J. Warburton, D. E. Alburger, C. J. Lister, and D. J. Millener, Nucl. Phys. A373, 13 (1982).

[60]E. J. Ansaldo, C. Rangacharylulu, D. Bender, U. Kramer, A. Richter, E. Spamer, and W. Knupfer, Phys. Lett. 95B, 31 (1980).

[61]J. Asher, J. R. Beene, M. A. Grace, W. L. Randolph, and D. F. H. Start, J. Phys. G 1, 415 (1975).

[62]J. Billowes, N. A. Jelley, O. L. Avila, and E. G. Adelberger, private communication.

[63]B. A. Brown, D. J. Millener, and I. S. Towner (unpublished).

[64]H. T. Fortune, J. Phys. G 4, L103 (1978).

[65]P. V. Hewka, C. H. Holbrow, and R. Middleton, Nucl. Phys. 88, 61 (1966).

[66]H. Freiesleben and R. Weisezahn, Nucl. Phys. A184, 273 (1972).